DOI: 10.1002/chem.200600686

Platinum(II) Complexes with π-Conjugated, Naphthyl-Substituted, Cyclometalated Ligands (RC^N^N): Structures and Photo- and Electroluminescence

Steven C. F. Kui,[a] Iona H. T. Sham,[a] Cecil C. C. Cheung,[a] Chun-Wah Ma,[a] Beiping Yan,[a] Nianyong Zhu,[a] Chi-Ming Che,*[a] and Wen-Fu Fu[b]

Abstract: The crystal structures and photophysical properties of mononuclear $[(RC^N^N)PtX](ClO_4)_n$ ((RC^N^N) = 3-(6′-(2″-naphthyl)-2′-pyridyl)isoquinolinyl and derivatives; X = Cl, $n = 0$; X = PPh_3 or PCy_3, $n = 1$), dinuclear $[(RC^N^N)_2Pt_2(\mu\text{-dppm})](ClO_4)_2$ (dppm = bis(diphenyphosphino)methyl) and trinuclear $[(RC^N^N)_3Pt_3(\mu\text{-dpmp})](ClO_4)_3$ (dpmp = bis(diphenylphosphinomethyl)phenylphosphine) complexes are presented. The crystal structures show extensive intra- and/or intermolecular π···π interactions; the two (RC^N^N) planes of $[(RC^N^N)_2Pt_2(\mu\text{-dppm})](ClO_4)_2$ (R = Ph, 3,5-tBu_2Ph or 3,5-$(CF_3)_2$Ph) are in a nearly eclipsed configuration with torsion angles close to 0°. [(RC^N^N)PtCl], $[(RC^N^N)_2Pt_2(\mu\text{-dppm})](ClO_4)_2$, and $[(RC^N^N)_3Pt_3(\mu\text{-dpmp})](ClO_4)_3$ are strongly emissive with quantum yields of up to 0.68 in CH_2Cl_2 or MeCN solution at room temperature. The [(RC^N^N)PtCl] complexes have a high thermal stability (T_d = 470–549 °C). High-performance light-emitting devices containing [(RC^N^N)PtCl] (R = H or 3,5-tBu_2Ph) as a light-emitting material have been fabricated; they have a maximum luminance of 63000 cd m^{-2} and CIE 1931 coordinates at $x = 0.36$, $y = 0.54$.

Keywords: electroluminescence · OLEDs · photoluminescence · pi interactions · platinum

Introduction

Platinum(II) complexes containing aromatic *N*-donor and/or cyclometalated ligands are known to display a variety of emissive excited states, including ligand-field (LF), metal-to-ligand charge transfer (MLCT), intraligand (IL) π–π*, excimeric σ*(π)→σ(π*), and oligomeric metal–metal-to-ligand charge-transfer (MMLCT) dσ*(dz^2)→σ(π*) ones.[1–17] The relative energy of these excited states is strongly affected by subtle changes in the local environment in which the Pt^{II} complex is located.[1,3,5–11,16,17] Of particular interest is the interplay between ^{3}MLCT/^{3}IL and ^{3}MMLCT emissive excited states, which are strongly affected by Pt^{II}–Pt^{II} and/or ligand–ligand interactions.[12,13,16–18] Several classes of diplatinum(II) complexes of the type $[Pt_2(tpy)_2(\mu\text{-L})]^{n+}$, $[Pt_2(C^N^N)_2(\mu\text{-L})]^{n+}$ and [(C^N)Pt(μ-pz)$_2$Pt(C^N)] (tpy = 2,2′:6′,2″-terpyridyl; (C^N^N) = 6-phenyl-2,2′-bipyridyl; L = guanidine, pyrazole, azaindole, diphenylformamidine, arginine or bis(diphenyphosphino)methyl; (C^N) = 2-(2,4-difluorophenyl)pyridyl; pz = pyrazolate derivatives) with intramolecular Pt–Pt contacts ranging from 2.998 to 3.432 Å are known to be emissive.[4,13,17–20] However, except for [(C^N)Pt(μ-pz)$_2$Pt(C^N)],[4] the ^{3}MMLCT excited states of most reported dinuclear Pt^{II} complexes have a relatively low emission quantum yield and short lifetime in solution at room temperature.[9,13,17,20]

In the course of our studies on [(C^N^N)PtX] complexes ((C^N^N) = 6-phenyl-2,2′-bipyridyl, X = Cl, PPh_3, acetylide, etc.), we have observed that: 1) the (C^N^N) ligand shows a strong preference for a planar geometry and can therefore be expected to disfavor the excited-state distortion that pro-

[a] Dr. S. C. F. Kui, Dr. I. H. T. Sham, C. C. C. Cheung, C.-W. Ma, Dr. B. Yan, Dr. N. Zhu, Prof. C.-M. Che
Department of Chemistry and the HKU-CAS Joint Laboratory on New Materials
The University of Hong Kong, Pokfulam Road
Hong Kong Special Administrative Region (China)
Fax: (+852) 2857-1586
E-mail: cmche@hku.hk

[b] Prof. Dr. W.-F. Fu
Technical Institute of Physics and Chemistry
Chinese Academy of Science
Peking 100101 (China)

Supporting Information for this article is available on the WWW under http://www.chemeurj.org/ or from the author.

motes radiationless decay;[11,21] 2) the π-conjugation and strong σ-donor strength of the deprotonated carbon donor of the (C^N^N) ligand increase the energy gap between the d–d and MLCT excited states;[21–24] and 3) the ability to vary the ancillary ligand X and ease of modification of the (C^N^N) ligand are advantageous for structural modification of [(C^N^N)PtX] complexes with tuneable photophysical properties.[12,13,15,16,19,20] We therefore envisioned that the intra- and intermolecular interactions between $[(C^N^N)Pt]^+$ moieties could be varied by enhancing noncovalent π···π interactions through the use of extended π-conjugated cyclometalated ligands.[16,25] In this work, we have replaced the 6-phenyl-2,2′-bipyridyl (C^N^N) ligand with 3-(6′-(2″-naphthyl)-2′-pyridyl)isoquinolinyl ligands (denoted as (RC^N^N) hereafter; Figure 1). The use of extended π-conjugated aromatic diimine ligands has been reported to lead to a relatively long-lived ^{3}MLCT excited state, as in the case of $[Ru(dqpy)dtp]^+$ (dqpy = 2,6-diisoquinolyl-(4-tolyl)pyridyl; dtpH = 2,9-bis(*p*-tolyl)-1,10-phenanthroline).[26] Here, the synthesis, crystal structures and emissive properties of the mononuclear 3-(6′-(2″-naphthyl)-2′-pyridyl)isoquinolinyl complexes $[(RC^N^N)PtX](ClO_4)_n$ (X = Cl, $n = 0$, **1a–1f**; X = PPh_3, $n = 1$, **3c**; X = PCy_3 (Cy = cyclohexyl), $n = 1$, **4b** and **4c**), the dinuclear complexes $[(RC^N^N)_2Pt_2(\mu\text{-dppm})](ClO_4)_2$ (dppm = bis(diphenyphosphino)methyl, **2a–2f**) as well as the trinuclear complexes $[(RC^N^N)_3Pt_3(\mu\text{-dpmp})](ClO_4)_3$ (dpmp = bis(diphenylphosphinomethyl)phenylphosphine, **5b** and **5d**; Figure 1) are reported. Complexes **1a** and **1d** have been tested for the fabrication of OLEDs.

Results and Discussion

The series of (RC^N^NH) ligands **a–f** was synthesized with product yields of 55–88%. Attempts to prepare [(RC^N^N)PtCl] by the reaction of (RC^N^NH) with K_2PtCl_4 in acetonitrile solution[27] were unsuccessful. However, we found that if glacial acetic acid was used as the solvent, **1a–1f** could be obtained in yields of up to 92% (Scheme 1). The mononuclear complexes **3c**, **4b** and **4c**, dinuclear complexes **2a–2f**, and trinuclear complexes **5b** and **5d** were obtained by stirring [(RC^N^N)PtCl] with the re-

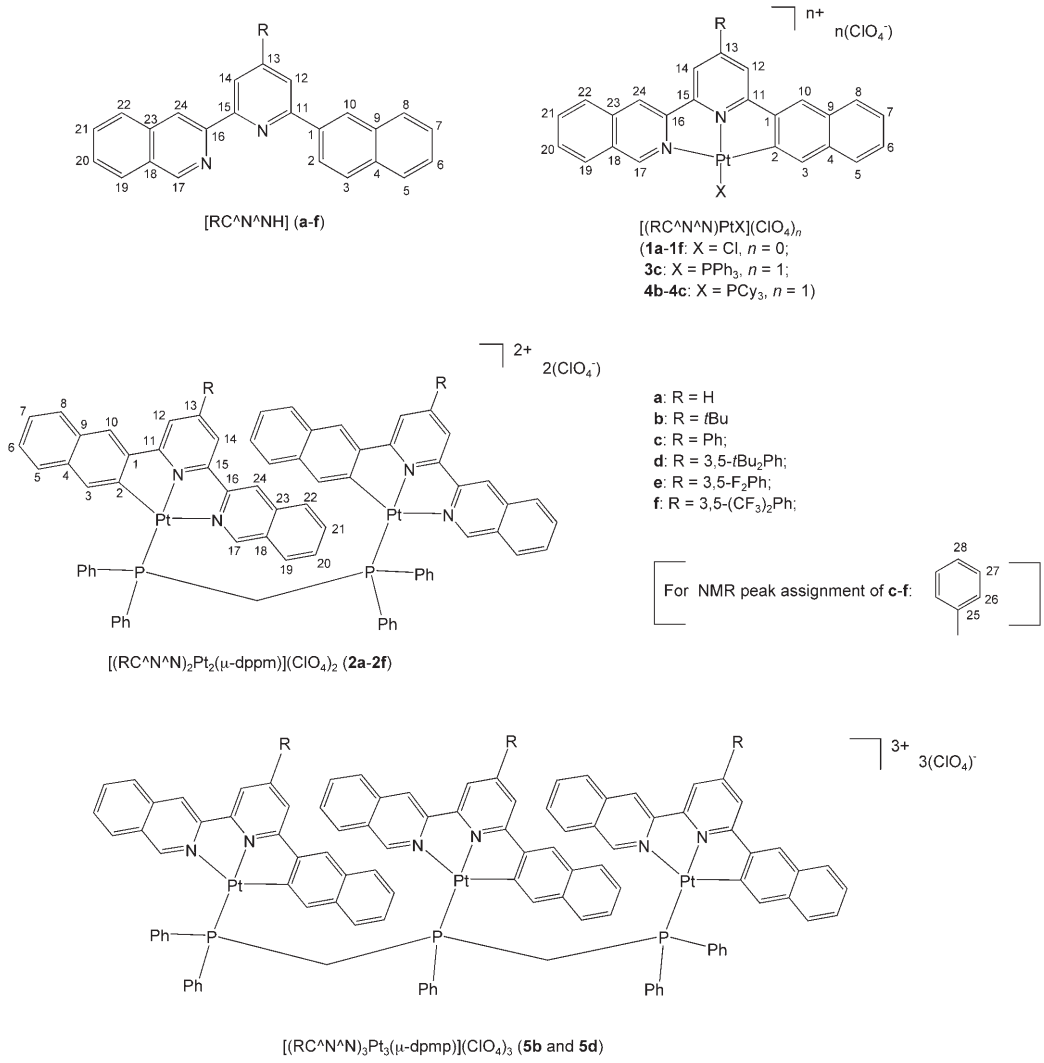

Figure 1. Structures and numbering scheme of ligands **a–f** as well as complexes **1a–1f**, **2a–2f**, **3c**, **4b**, **4c**, **5b** and **5d** for NMR peak assignment.

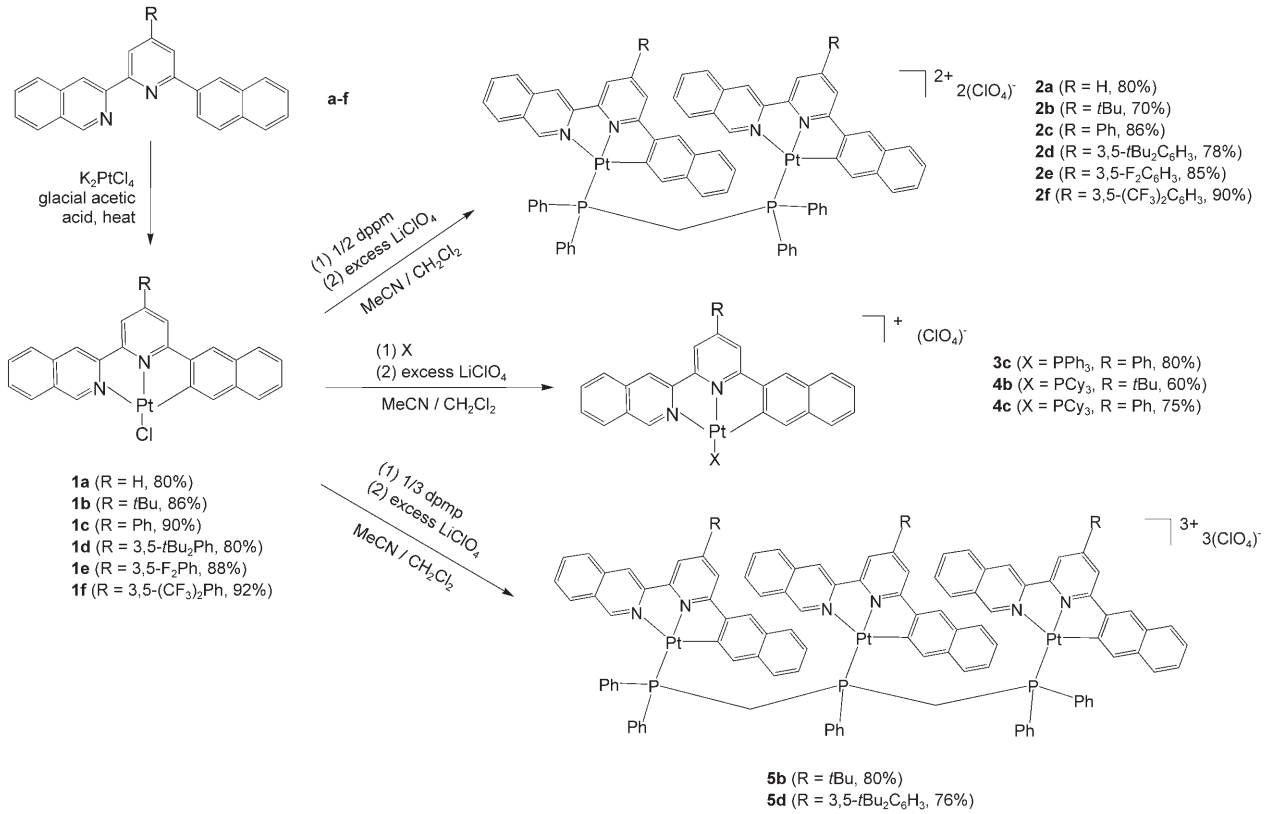

Scheme 1. The synthesis of **1a–1f**, **2a–2f**, **3c**, **4b**, **4c**, and **5b**. The X and R groups and yields are given in parentheses.

spective PPh_3, PCy_3, dppm, or dpmp ligand in a MeCN/CH_2Cl_2 solution (Scheme 1); they were isolated as ClO_4^- salts.

Physical characterizations: The FAB-mass spectra reveal prominent molecular ion [M^+] peaks for **1a–1f**, a [$M-ClO_4$]$^+$ peak for **3c**, **4b**, and **4c**, [$M-ClO_4$]$^+$ or [$M-2(ClO_4)$]$^+$ peaks for **2a–2f**, and [$M-ClO_4$]$^+$, [$M-2(ClO_4)$]$^+$, or [$M-3(ClO_4)$]$^+$ peaks for **5b** and **5d**. The atom numbering scheme of ligands **a–f** and complexes **1a–1f**, **2a–2f**, **3c**, **4b**, **4c**, **5b** and **5d** for NMR peak assignments are depicted in Figure 1. The spatial relationship of the protons in the [(RC^N^N)PtCl] complexes was assigned based on the results of ^{1}H–^{1}H correlation and NOESY 2D NMR experiments.

The ^{31}P NMR spectra of **2a–2f** show one intense signal with ^{195}Pt satellites ($^1J_{P,Pt}\approx4250$ Hz). Similar findings have previously been obtained for [(C^N^N)$_2$Pt$_2$(μ-dppm)]-(ClO_4)$_2$ ($^1J_{P,Pt}\approx4110$ Hz),[16,18,20] [(C^N^C)$_2$Pt$_2$(μ-dppm)] ((C^N^C)=2,6-diphenylpyridyl and derivatives; $^1J_{P,Pt}\approx4150$ Hz)[28] and [(RC^N^C)$_2$Pt$_2$(μ-dppm)] ((RC^N^C)=2,6-di-(2′-naphthyl)pyridyl and derivatives; $^1J_{P,Pt}\approx4250$ Hz).[25] There is a close match between the ^{31}P NMR spectrum of **2d** and the simulated spectrum based on an AA′XX′ system[29] ($^1J_{P,Pt}=4200$ and $^2J_{P,Pt}=80$ Hz). The two phosphorus atoms of the Pt-P-CH$_2$-P-Pt bridge in **2a–2f** are indistinguishable at room temperature; however, broadening of the signals was observed in deuterated MeCN as the temperature was lowered from 0 to −45 °C. No fluxional behavior was observed for **2a–2f**.

The ^{31}P NMR spectrum of **5d** reveals two signals at $\delta=$ 9.7 (central) and 11.7 ppm (terminal) with ^{195}Pt satellites ($^1J_{P,Pt}=4042$ and 4094 Hz, respectively), and its ^{195}Pt-{^{31}P} NMR spectrum shows two doublets at $\delta=-3727.8$ (central) and −3886.5 ppm (terminal) with $^1J_{P,Pt}=3995$ and 4070 Hz, respectively. The NMR spectroscopic data are consistent with two chemically inequivalent phosphorus atoms in **5d**.[16]

Thermogravimetric analysis (TGA) revealed that the [(RC^N^N)PtCl] complexes **1a–1f** decompose at temperatures above 470 °C ($T_d=470$–549 °C, Table 1). The mononuclear complexes with PPh_3 or PCy_3 ligands (**3c**, **4b** and **4c**) have a lower T_d (320–376 °C) than their Cl congeners **1a–1f**. The dinuclear complexes **2a–2f** decompose above 370 °C ($T_d=376$–385 °C) and the trinuclear complexes **5b** and **5d** decompose at 421 and 337 °C, respectively (Table 1). No glass transition was observed in differential scanning calorimetric (DSC) studies for **1a–1f** and **2a–2f** in scans up to 400 °C, thus indicating that the glass-transition temperatures (T_g) of these complexes are above 400 °C.

Cyclic voltammetry: The electrochemical data of **1a–1f**, **2a–2f**, **3c**, **4b**, **4c**, **5b**, and **5d** are summarized in Table 1. The cyclic voltammograms of **1d** and **2d** are depicted in

Table 1. Thermogravimetric and electrochemical data[a] of **1a**–**1f**, **2a**–**2f**, **3c**, **4b**, **4c**, **5b** and **5d**.

Complex	T_d[b] [°C]	Reduction $E_{1/2}$ [V][c]	Quasi-reversible couple[c]	Anodic peak E_{pa} [V][c]
1a	470	−1.76	–	0.44
1b	484	−1.86	–	0.54
1c	509	−1.73	–	0.45
1d	532	−1.73	–	0.58
1e	479	−1.70	–	0.37
1f	549	−1.66	–	0.56
2a	385	−1.48	−1.67	–
2b	378	−1.52	−1.75	–
2c	376	−1.43	−1.69	–
2d	380	−1.51	−1.69	–
2e	379	−1.32, −1.53	–	–
2f	381	−1.28, −1.48	–	–
3c	376	−1.52	–	–
4b	320	−1.60	–	–
4c	349	−1.55	–	–
5b	421	−1.68	–	0.53
5d	337	−1.44, −1.62	–	0.63

[a] Determined in DMF at 298 K with 0.1 M nBu_4NPF_6 as the supporting electrolyte; scan rate = 50 mV s^{-1}. [b] Decomposition temperature. [c] Value versus $E_{1/2}$ ($Cp_2Fe^{+/0}$) (0.11–0.13 V versus $Ag/AgNO_3$ (0.1 M in MeCN) reference electrode).

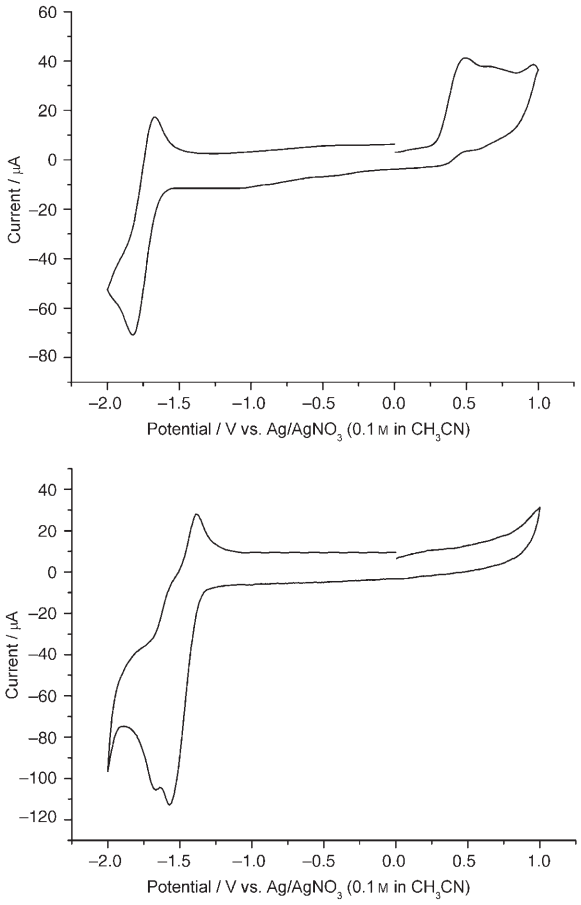

Figure 2. Cyclic voltammograms of **1d** (top, 10^{-4} M) and **2d** (bottom, 10^{-4} M) in DMF containing 0.1 M $nBuNPF_6$ as supporting electrolyte at 298 K. Scan rate: 50 mV s^{-1}.

Figure 2. Complexes **1a**–**1f**, **3c**, **4b**, and **4c** show one reversible reduction couple ($E_{1/2} = -1.52$ to -1.86 V versus $[Cp_2Fe]^{+/0}$) in DMF solution at 298 K; this couple presumably corresponds to reduction of the (RC^N^N) ligand. The $E_{1/2}$ of this reduction couple for **1b** occurs at -1.86 V, while it is anodically shifted to -1.66 V for **1f** due to the electron-withdrawing 3,5-(CF_3)Ph substituent on the (RC^N^N) ligand. Complexes **1a**–**1f** show an irreversible oxidation wave in the range $E_{pa} = 0.37$–0.58 V versus $Cp_2Fe^{+/0}$.

The dinuclear complexes **2a**–**2d** show two reduction couples in the ranges $E_{1/2} = -1.43$ to -1.52 (reversible) and -1.67 to -1.75 V (quasi-reversible), respectively, versus $[Cp_2Fe]^{+/0}$. The trinuclear complex **5b** shows one reversible reduction couple at $E_{1/2} = -1.68$ V, whereas **5d** shows two reversible couples at $E_{1/2} = -1.44$ and -1.62 V, respectively. These reduction couples are presumably ligand-centered. The observation of two reversible reduction couples for the dinuclear and trinuclear Pt^{II} complexes, whereas only one ligand-centered reduction couple is observed for its mononuclear congeners, suggests coupling between the [(RC^N^N)Pt] units upon reduction.[13,16,20]

Crystal structures: X-ray crystal data[30] as well as selected bond distances and angles for **1a**, **1c**, **2a**–**2d**, **2f**, **3c**, **4b**, **4c**, and **5b** are listed in Table 2 and Table 3, respectively. Perspective views are depicted in the figures below. The coordination geometries of **1a**, **1c**, **3c**, **4b**, and **4c** (Figure 3) are similar to that of the 6-phenyl-2,2′-bipyridyl congener [(C^N^N)PtCl]. In each case, the Pt atom adopts a distorted square-planar geometry, as revealed by the N(1)-Pt(1)-C(1) angle of 163.1(3)° in **1a**, the N(1)-Pt(1)-C(16) angle of 163.1(8)° in **1c**, the N(1)-Pt(1)-C(1) angle of 158.4(5)° in **3c**, the N(2)-Pt(1)-C(16) angle of 156.3(2)° in **4b** and the N(2)-Pt(1)-C(1) angle of 156.6(2)° in **4c**; these angles deviate significantly from 180°. The coordinating O, N, Pt and Cl atoms in **1a** and **1c** are close to co-planar, with the Cl atom lying out of the plane by only 3.6° and 2.2°, respectively. On the other hand, the PPh_3 or PCy_3 groups of **3c**, **4b** and **4c** lie out of the plane by 7.0°, 19.6° and 14.1°, respectively. We suggest that intermolecular π···π interactions between neighboring $[(RC^N^N)Pt(PR_3)]^+$ molecules would be enhanced by bending of the phosphine ligand out of the Pt^{II} coordination plane such that the (RC^N^N) planes are in proximity. The Pt–N distances in **1a**, **1c**, **3c**, **4b** and **4c** are 1.9–2.2 Å (Table 3); these values are comparable to those in $[(C^N^N)Pt(PPh_3)]ClO_4$ ((C^N^N) = 6-phenyl-2,2′-bipyridyl; Pt–N = 1.985 and 2.12 Å),[20] $[(O^N^N)PtCl]\cdot CH_2Cl_2$ ((O^N^N) = 6-(2-hydroxyphenyl)-2,2′-bipyridyl; 2.00 Å),[31] [(*t*BuO^N^N)PtCl] ((*t*BuO^N^N) = 4,4′-di-*tert*-butyl-6-(2-hydroxyphenyl)-2,2′-bipyridyl; 1.979 and 2.006 Å)[32] and [Pt-(N_2O_2)] ($H_2(N_2O_2)$ = bis(2′-phenol)bipyridine or -phenanthroline; 1.960 and 1.978 Å).[33] The Pt–Cl distances in **1a** (2.3136 Å) and **1c** (2.314 Å) resemble those of [(O^N^N)PtCl] and [(*t*BuO^N^N)PtCl] (2.3 Å).[31,32] For **3c**, **4b**, and **4c**, the Pt–P (2.253, 2.2826 and 2.2971 Å, respectively) and Pt–C distances (2.001, 2.054 and 2.041 Å, respectively) are similar to those in $[(C^N^N)Pt(PPh_3)]ClO_4$ (Pt–

Table 2. Crystal data of **1a**, **1c**, **2a**–**2d**, **2f**, **3c**, **4b**, **4c**, and **5b**.

Complex	**1a**	**1c**	**3c**	**4b**	**4c**
formula	$C_{24}H_{15}ClN_2Pt\cdot CHCl_3$	$C_{30}H_{19}ClN_2Pt\cdot 2.5\,CHCl_3$	$C_{48}H_{33}ClN_2O_4PPt\cdot CH_3OH$	$C_{46}H_{56}ClN_2O_4PPt\cdot 2\,CH_3CN$	$C_{48}H_{52}ClN_2O_4PPt\cdot 0.5\,CH_3CN$
FW	681.29	936.43	995.32	1044.55	1002.95
color	yellow	yellow	yellow	yellow	yellow
crystal size [mm^3]	0.6×0.15×0.1	0.50×0.10×0.06	0.35×0.15×0.06	0.3×0.2×0.2	0.4×0.35×0.2
crystal system	monoclinic	triclinic	triclinic	monoclinic	monoclinic
space group	$P2_1/n$	$P\bar{1}$ (no. 2)	$P\bar{1}$ (no. 2)	$P2_1/n$	$C2/c$
a [Å]	7.926(2)	10.306(2)	10.713(2)	16.423(3)	26.188(5)
b [Å]	19.361(4)	14.437(3)	13.300(3)	17.976(4)	14.708(3)
c [Å]	15.290(3)	24.212(5)	16.081(3)	17.270(4)	24.052(5)
α [°]	90	98.21(3)	71.77(3)	90	90
β [°]	100.28(3)	100.58(3)	75.45(3)	110.42(3)	99.88(3)
γ [°]	90	96.48(3)	77.53(3)	90	90
V [Å^3]	2308.7(8)	3468.9(12)	2082.8(7)	4778.1(18)	9127(3)
Z	4	4	2	4	8
ρ_{calcd} [g cm^{-3}]	1.960	1.793	1.587	1.452	1.460
μ [mm^{-1}]	6.558	4.726	3.522	3.073	3.214
$F(000)$	1304	1812	990	2128	4056
$2\theta_{max}$ [°]	50.98	47.4	45.00	51.24	50.68
no. unique data	4003	5398	2839	8321	7091
Gof [F^2]	1.06	0.89	0.730	0.833	0.92
R[a]	0.040	0.061	0.049	0.035	0.031
R_w[b]	0.102	0.11	0.103	0.072	0.076
residual ρ [e Å^{-3}]	1.389, −1.314	1.276, −0.970	0.808, −0.597	0.851, −1.458	0.594, −0.602
CCDC number	601687	287984	287987	287985	287988

Complex	**2a**	**2b**	**2c**	**2d**	**2f**	**5b**
formula	$C_{73}H_{52}Cl_2N_4O_8P_2Pt_2\cdot 0.5\,CH_3CN\cdot H_2O$	$C_{81}H_{68}Cl_2N_4O_8P_2Pt_2\cdot 2\,CH_3CN$	$C_{85}H_{60}Cl_2N_4O_8P_2Pt_2\cdot 3\,CH_3CN$	$C_{101}H_{92}Cl_2N_4O_8P_2Pt_2\cdot 2\,CH_2Cl_2\cdot C_4H_{10}O$	$C_{89}H_{56}Cl_2F_{12}N_4O_8P_2Pt_2\cdot 6\,CH_2Cl_2$	$C_{116}H_{98}Cl_3N_6O_{12}P_3Pt_3\cdot 2\,CH_3CN$
FW	1674.75	1830.52	1910.54	2256.78	2569.95	2634.64
color	yellow	yellow	yellow	orange	orange	yellow
crystal size [mm^3]	0.30×0.20×0.15	0.35×0.30×0.25	0.35×0.20×0.10	0.50×0.25×0.10	0.40×0.15×0.12	0.35×0.3×0.2
crystal system	monoclinic	monoclinic	triclinic	monoclinic	monoclinic	orthorhombic
space group	$P2_1/c$	$C2/c$	$P\bar{1}$ (no. 2)	$P2_1/n$	$C2/c$	$P2_12_12_1$
a [Å]	23.309(5)	13.315(3)	12.435(3)	15.672(3)	22.067(4)	14.402(3)
b [Å]	14.645(3)	27.131(5)	15.434(3)	34.206(7)	25.992(5)	19.809(4)
c [Å]	19.144(4)	21.041(4)	22.325(5)	19.870(4)	18.102(4)	38.566(8)
α [°]	90	90	108.25(3)	90	90	90
β [°]	94.91(3)	98.47(3)	93.07(3)	106.16(3)	100.99(3)	90
γ [°]	90	90	105.80(3)	90	90	90
V [Å^3]	6511(2)	7518(3)	3869.9(15)	10231(4)	10192(4)	11002(4)
Z	4	4	2	4	4	4
ρ_{calcd} [g cm^{-3}]	1.708	1.617	1.640	1.465	1.675	1.591
μ [mm^{-1}]	4.487	3.893	3.786	2.977	3.218	3.987
$F(000)$	3292	3640	1894	4544	5048	5224
$2\theta_{max}$ [°]	50.64	50.90	50.98	51.10	50.68	48.80
no. unique data	7641	6490	12856	12371	8066	14453
Gof [F^2]	0.87	1.08	0.93	0.81	0.93	0.596
R[a]	0.049	0.037	0.042	0.050	0.046	0.037
R_w[b]	0.11	0.044	0.062	0.114	0.072	0.082
residual ρ [e Å^{-3}]	1.083, −1.221	1.164, −1.653	1.222, −0.861	1.073, −1.041	0.839, −1.057	0.664, −0.614
CCDC number	287990	287992	287986	287991	287987	601688

[a] $R=\Sigma||F_o|-|F_c||/\Sigma|F_o|$. [b] $R_w=[\Sigma w(|F_o|-|F_c|)^2/\Sigma w|F_o|^2]^{1/2}$.

P = 2.243, Pt–C = 2.00 Å).[20] In the crystal structures of **1a**, **1c**, **3c**, **4b** and **4c**, the molecules are oriented in pairs *anti* to each other, with an intermolecular π···π stacking distance of about 3.5 Å and Pt···Pt distances greater than 4 Å.

Complexes **2a**–**2d** and **2f** consist of two (RC^N^N)Pt units bridged by a dppm ligand (Figure 4), while the three (RC^N^N)Pt moieties in **5b** are bridged by a dpmp ligand (Figure 5). The Pt–N, Pt–P and Pt–C distances (2.0–2.2, 2.2–2.3 and 2.0–2.1 Å, respectively; Table 3) in these complexes are similar to those in $[(C^N^N)_2Pt_2(\mu\text{-dppm})](ClO_4)_2$ (Pt–N = 1.985 and 2.12, Pt–P = 2.248 and Pt–C = 2.024 Å).[20] The intramolecular Pt···Pt distance of 3.165(1) Å in **2a** is slightly shorter than those in $[(C^N^N)_2Pt_2(\mu\text{-dppm})](ClO_4)_2$ (3.270),[13,16,18,20] $[(C^N^N)_2Pt_2(\mu\text{-dppm})](ClO_4)_2\cdot 5H_2O$ (3.245),[13,16,18,20] $[(C^N^N)_3Pt_3(\mu\text{-dpmp})](ClO_4)_3\cdot H_2O$ (3.190 and 3.399), $[(C^N^N)_3Pt_3(\mu\text{-dpmp})](ClO_4)_3\cdot 2Et_2O\cdot CH_3CN$

Table 3. Selected bond lengths [Å] and angles [°] for **1a**, **1c**, **2a**–**2d**, **2f**, **3c**, **4b**, **4c**, and **5b**.

					1a				
Pt(1)−C(1)	2.088(5)	Pt(1)−N(1)	1.997(8)	Pt(1)−N(2)	1.958(5)	Pt(1)−Cl(1)	2.314(2)		
N(2)-Pt(1)-C(1)	80.1(2)	N(2)-Pt(1)-N(1)	83.0(3)	N(1)-Pt(1)-C(1)	163.1(3)	N(2)-Pt(1)-Cl(1)	176.4(2)	C(1)-Pt(1)-Cl(1)	96.9(2)
N(1)-Pt(1)-Cl(1)	99.9(2)								
					1c				
Pt(1)−C(16)	2.08(2)	Pt(1)−N(1)	2.12(2)	Pt(1)−N(2)	1.94(2)	Pt(1)−Cl(1)	2.314(6)		
C(16)-Pt(1)-N(2)	80.9(7)	N(1)-Pt(1)-N(2)	82.2(8)	N(1)-Pt(1)-C(16)	163.1(8)	N(2)-Pt(1)-Cl(1)	177.8(5)	Cl(1)-Pt(1)-C(16)	97.4(5)
Cl(1)-Pt(1)-N(1)	99.5(6)								
					2a				
Pt(1)−C(1)	2.04(1)	Pt(1)−N(1)	2.12(1)	Pt(1)−N(2)	2.00(1)	Pt(1)−P(1)	2.245(4)	Pt(2)−C(25)	2.02(2)
Pt(2)−N(3)	2.16 (1)	Pt(2)−N(4)	2.04(1)	Pt(2)−P(2)	2.252(4)	Pt(1)···Pt(2)	3.165(1)		
C(1)-Pt(1)-N(2)	81.6(5)	N(1)-Pt(1)-N(2)	77.4(5)	C(1)-Pt(1)-P(1)	94.8(5)	N(1)-Pt(1)-P(1)	105.9(3)	C(25)-Pt(2)-N(4)	82.7(5)
N(3)-Pt(2)-N(4)	77.8(5)	C(25)-Pt(2)-P(2)	96.1(4)	N(3)-Pt(2)-P(2)	103.4(4)	Pt(1)-P(1)-P(2)-Pt(2)	16.3(1)		
					2b				
Pt(1)−C(16)	2.007(5)	Pt(1)−N(1)	2.158(4)	Pt(1)−N(2)	2.024(4)	Pt(1)−P(1)	2.248(1)	Pt(1)···Pt(1*)	3.198(7)
C(16)-Pt(1)-N(2)	81.8(2)	N(1)-Pt(1)-N(2)	77.9(2)	C(16)-Pt(1)-P(1)	94.5(2)	N(1)-Pt(1)-P(1)	105.7(2)	Pt(1)-P(1)-P(1*)-Pt(1*)	29.69(5)
					2c				
Pt(1)−C(16)	2.010(8)	Pt(1)−N(1)	2.150(6)	Pt(1)−N(2)	2.017(6)	Pt(1)−P(1)	2.243(2)	Pt(2)−C(46)	2.032(7)
Pt(2)−N(3)	2.166(6)	Pt(2)−N(4)	2.049(6)	Pt(2)−P(2)	2.261(2)	Pt(1)···Pt(2)	3.37(4)		
C(16)-Pt(1)-N(2)	81.8(3)	N(1)-Pt(1)-N(2)	77.7(2)	C(16)-Pt(1)-P(1)	94.6(2)	N(1)-Pt(1)-P(1)	105.7(2)	C(46)-Pt(2)-N(4)	80.5(3)
N(3)-Pt(2)-N(4)	77.5(2)	C(46)-Pt(2)-P(2)	96.5(2)	N(3)-Pt(2)-P(2)	105.4(2)	Pt(1)-P(1)-P(2)-Pt(2)	1.82(8)		
					2d				
Pt(1)−C(1)	2.05(1)	Pt(1)−N(1)	2.167(9)	Pt(1)−N(2)	2.015(9)	Pt(1)−P(1)	2.261(3)	Pt(2)−C(39)	2.00(1)
Pt(2)−N(3)	2.15(1)	Pt(2)−N(4)	2.027(9)	Pt(2)−P(2)	2.247(3)	Pt(1)···Pt(2)	3.29(6)		
C(1)-Pt(1)-N(2)	82.2(4)	N(1)-Pt(1)-N(2)	77.2(4)	C(1)-Pt(1)-P(1)	93.7(3)	N(1)-Pt(1)-P(1)	107.0(3)	C(39)-Pt(2)-N(4)	81.7(4)
N(3)-Pt(2)-N(4)	77.9(4)	C(39)-Pt(2)-P(2)	95.9(3)	N(3)-Pt(2)-P(2)	104.5(2)	Pt(1)-P(1)-P(2)-Pt(2)	0.2(1)		
					2f				
Pt(1)−C(1)	2.031(8)	Pt(1)−N(1)	2.034(6)	Pt(1)−N(2)	2.152(6)	Pt(1)−P(1)	2.255(2)	Pt(1)···Pt(2)	3.28(4)
C(1)-Pt(1)-N(1)	81.8(3)	N(1)-Pt(1)-N(2)	77.2(2)	C(1)-Pt(1)-P(1)	94.9(2)	N(2)-Pt(1)-P(1)	106.0(2)	Pt(1)-P(1)-P(1*)-Pt(2*)	0.20(7)
					3c				
Pt(1)−C(1)	2.00(2)	Pt(1)−N(1)	2.13(1)	Pt(1)−N(2)	1.976(6)	Pt(1)−P(2)	2.253(4)	C(1)-Pt(1)-N(2)	96.4(5)
N(2)-Pt(1)-N(1)	77.8(4)	N(2)-Pt(1)-C(1)	81.1(5)	N(2)-Pt(1)-P(2)	173.1(3)	C(1)-Pt(1)-P(2)	96.4(5)	N(1)-Pt(1)-P(2)	105.1(3)
					4b				
Pt(1)−C(16)	2.054(5)	Pt(1)−N(1)	2.023(4)	Pt(1)−N(2)	2.103(4)	Pt(1)−P(1)	2.283(2)		
C(16)-Pt(1)-N(2)	156.3(2)	N(1)-Pt(1)-N(2)	78.6(2)	C(16)-Pt(1)-P(1)	102.4(2)	N(2)-Pt(1)-P(1)	101.2(1)	N(1)-Pt(1)-C(16)	79.6(2)
N(1)-Pt(1)-P(1)	160.7(1)								
					4c				
Pt(1)−C(1)	2.041(6)	Pt(1)−N(1)	2.028(4)	Pt(1)−N(2)	2.154(5)	Pt(1)−P(1)	2.297(1)		
C(1)-Pt(1)-N(2)	156.6(2)	N(1)-Pt(1)-N(2)	77.8(2)	C(1)-Pt(1)-P(1)	99.9(1)	N(2)-Pt(1)-P(1)	103.3(1)	N(1)-Pt(1)-C(1)	80.5(2)
N(1)-Pt(1)-P(1)	165.9(1)								
					5b				
Pt(1)−C(1)	2.01(1)	Pt(1)−N(1)	2.157(9)	Pt(1)−N(2)	2.019(9)	Pt(1)−P(1)	2.255(3)	Pt(2)−N(4)	2.024(8)
Pt(2)−C(29)	2.06(1)	Pt(2)−N(3)	2.172(8)	Pt(2)−P(2)	2.263(3)	Pt(3)−N(6)	2.035(8)	Pt(3)−C(57)	2.05(1)
Pt(3)−N(5)	2.163(9)	Pt(3)−P(3)	2.260(3)						
C(1)-Pt(1)-N(2)	81.0(4)	C(1)-Pt(1)-N(1)	159.1(4)	N(2)-Pt(1)-N(1)	78.2(3)	C(1)-Pt(1)-P(1)	100.0(3)	N(2)-Pt(1)-P(1)	173.2(3)
N(1)-Pt(1)-P(1)	100.9(2)	N(4)-Pt(2)-C(29)	81.5(4)	N(4)-Pt(2)-N(3)	76.0(3)	C(29)-Pt(2)-N(3)	157.2(3)	N(4)-Pt(2)-P(2)	174.3(3)
C(29)-Pt(2)-P(2)	95.0(3)	N(3)-Pt(2)-P(2)	107.7(2)	N(6)-Pt(3)-C(57)	80.5(4)	N(6)-Pt(3)-N(5)	77.9(3)	C(57)-Pt(3)-N(5)	158.5(3)
N(6)-Pt(3)-P(3)	175.6(3)	C(57)-Pt(3)-P(3)	98.4(3)	N(5)-Pt(3)-P(3)	103.1(2)				

(3.364 and 3.617), $[(t\text{BuC^N^N})_3Pt_3(\mu\text{-dpmp})](ClO_4)_3\cdot 3\,CH_3CN$ (3.217 and 3.601) and $[(Et_2OCC\text{^N^N})_3Pt_3(\mu\text{-dpmp})](ClO_4)_3\cdot 2\,Et_2O$ (3.466 and 3.647 Å).[16] In the dinuclear complexes, the intramolecular Pt···Pt contacts are in the order: **2a** (3.16(1)) < **2b** (3.198(7)) < **2f** (3.28(4)) < **2d** (3.29(6)) < **2c** (3.37(4) Å). These values fall in the range of intermetal separations normally observed for platinum(II) complexes containing an extended linear chain structure (3.09–3.50 Å). There is no close intermolecular Pt···Pt contact between adjacent $[(RC\text{^N^N})_2Pt_2(\mu\text{-dppm})]^{2+}$ molecules. In the trinuclear complex **5b**, the intramolecular Pt1···Pt2 contact of 3.53 Å, Pt2···Pt3 contact of 3.30 Å and the Pt1···Pt2···Pt3 angle of 163° are indicative of the presence of weak $d^8\cdots d^8$ and ligand–ligand interactions across Pt1···Pt2···Pt3. These values are similar to those in the trinuclear substituted (C^N^N) analogues $[(C\text{^N^N})_3Pt_3(\mu\text{-dpmp})](ClO_4)_3\cdot H_2O$ (3.36, 3.62 Å, 162°), $[(t\text{BuC^N^N})_3Pt_3(\mu\text{-dpmp})](ClO_4)_3\cdot 2\,Et_2O\cdot CH_3CN$ (3.22, 3.60 Å, 157°) and $[(EtO_2CC\text{^N^N})_3Pt_3(\mu\text{-dpmp})](ClO_4)_3\cdot 2\,CH_3CN$ (3.47, 3.64 Å, 162°).[16]

π···π Stacking is an important structural feature in metal complexes containing chelating aromatic N-donor ligands.[34] According to the Hunter–Sanders rules, an offset, slipped or parallel displaced staggered configuration is usually preferred over the face-to-face alignment of an eclipsed configura-

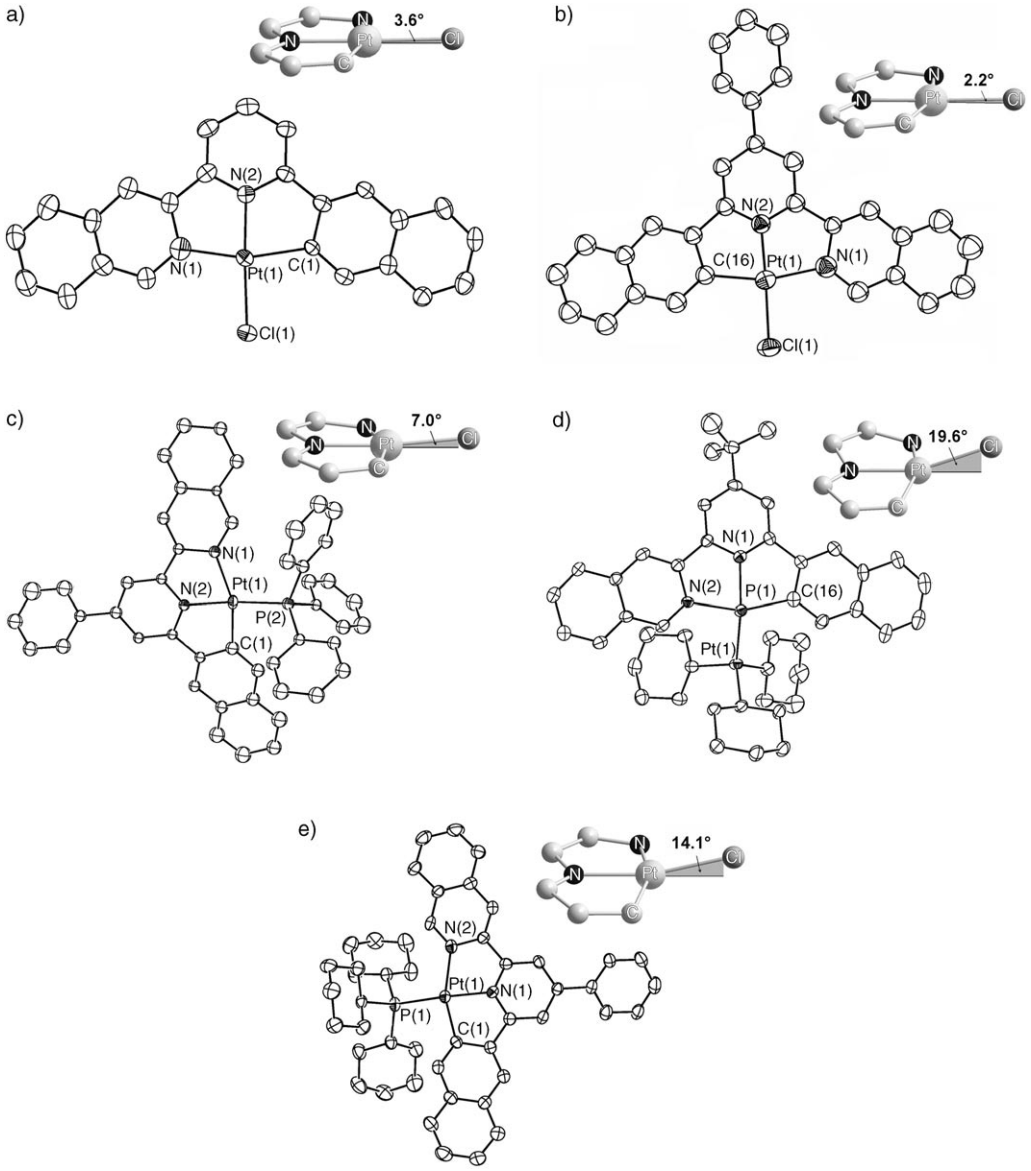

Figure 3. Molecular structures of a) **1a**, b) **1c** (torsion angle α(C11-C12-C25-C26) = 31°), c) **3c** (α(C12-C13-C25-C26) = 42°), d) **4b**, and e) **4c** (α(C12-C13-C25-C26) = 28°). The thermal ellipsoids are at 30% probability. All hydrogen atoms and solvent molecules have been omitted for clarity. The insets show the out-of-plane angle of Cl, PPh_3, or PCy_3.

tion in π-stacking aromatic moieties due to electrostatic repulsion.[35] Eclipsed π-stacking of aromatic moieties shows an increased stability when the aromatic moieties bear an electronegative atom such as nitrogen. In the literature, an eclipsed alignment in metal complexes containing multidentate N-donor ligands remains sparse.[34] In this work, the two (RC^N^N) planes in **2a** or **2b** adopt a staggered configuration such that a small deviation from co-planarity is observed. The interplanar distances of the Pt(RC^N^N) moieties, as estimated by the Pt···Pt separations of around 3.2 Å, are slightly shorter than those (3.4–4.6 Å) reported for most transition-metal pyridine or quinoline moieties[35] (such as (2,2′-bipyridyl-*N*,*N*′)dicyanoplatinum(II) and -palladium(II) (ca. 3.4 Å)[36] and 3,4,7,8-tetramethyl-1,10-phenanthroline)copper(I)–acetone solvate (ca. 3.7 Å)[37]) that are displaced in parallel at an angle of 16–40°.[35] The α(Pt-P-P-Pt) torsion angles, between the two staggered (RC^N^N)Pt moieties in **2a** and **2b** are 16.3(1)° and 29.69(5)°, respectively. These torsion angles are significantly smaller than that of 44.6° in the 6-phenyl-2,2′-bipyridyl congener $[(C^N^N)_2Pt_2(\mu\text{-dppm})]^{2+}$.[13,16,18,20] On the other hand, **2c**, **2d** and **2f** exhibit an almost eclipsed alignment of the two [(RC^N^N)Pt] planes, with estimated interplane distances of about 3.3–3.4 Å. The α(Pt-P-P-Pt) angles of **2c**, **2d** and **2f** are 1.82(8)°, 0.19(13)° and 0.20(7)° respectively; these angles are close to zero even though the complexes bear bulky R groups on the ligand (Ph in **2c**, 3,5-tBu$_2$Ph in **2d** and 3,5-$(CF_3)_2$Ph in **2f**). Thus, the two (RC^N^N)Pt units

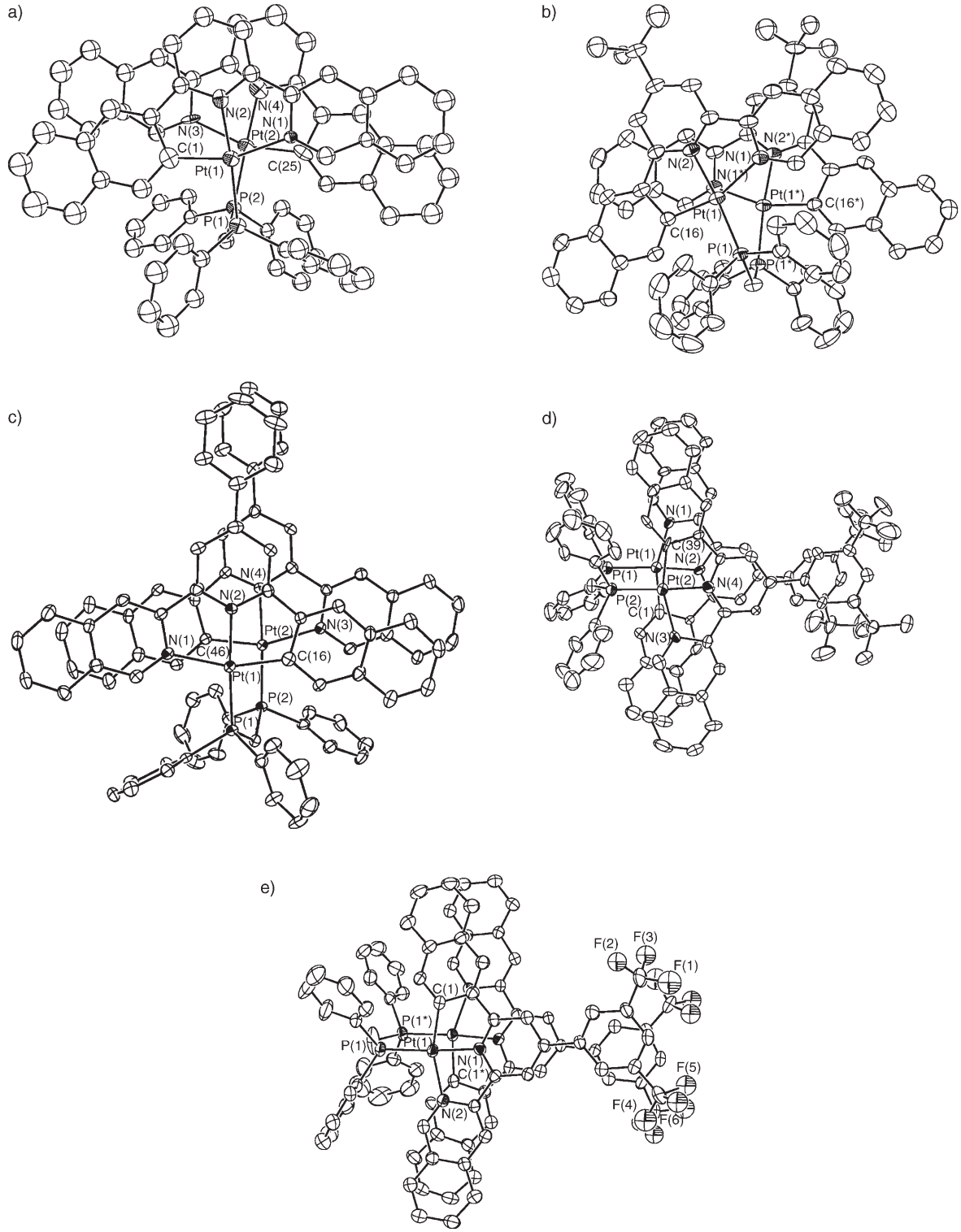

Figure 4. Molecular structures of a) **2a**, b) **2b**, c) **2c** (torsion angle α(C11-C12-C25-C26) = 21°), d) **2d** (α(C12-C13-C25-C26) = 31°), and e) **2f** (α(C12-C13-C25-C26) = 27°). The thermal ellipsoids are at 30% probability. All hydrogen atoms and solvent molecules have been omitted for clarity.

of these dinuclear Pt^{II} complexes are nearly parallel to each other and are related by a C_2 axis passing through the CH_2 moiety of the dppm ligand. We have observed previously that when the extent of π-conjugation in the cyclometalated ligand of dinuclear complexes (**2c**, **2d** and **2f**, where R involves a phenyl group) is increased, the extent of slipping or offset between the ligand planes is decreased (i.e. the preference for an eclipsed configuration is increased).

The three (RC^N^N)Pt units in **5b** are partially staggered, with α(Pt2-P-P-Pt3) and α(Pt1-P-P-Pt2) torsion

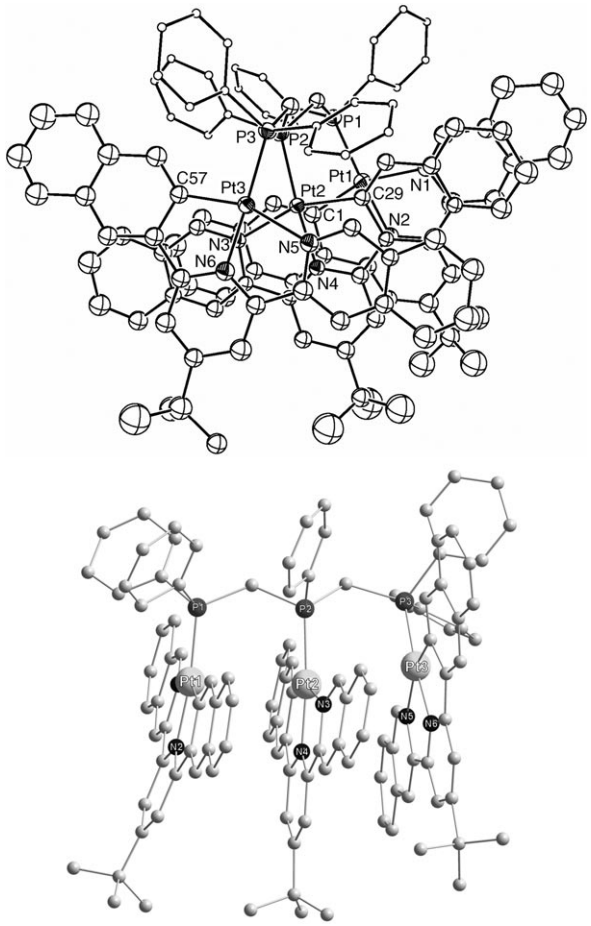

Figure 5. Molecular structure of **5b**. The thermal ellipsoids are at 30% probability. All hydrogen atoms and solvent molecules have been omitted for clarity. Top: View from the top; bottom: view from the side.

Table 4. Selected structural parameters regarding Pt···Pt interactions in dinuclear Pt^{II} complexes.

Complex	Pt···Pt distance [Å]	Torsion angle [°]	Pt1···Pt2···Pt3 angle [°]
$[(C\hat{}N\hat{}N)_2Pt_2(\mu\text{-dppm})]^{2+}$[a,b]	3.270	44.6	–
$[((4\text{-}MeC_6H_4)\text{-}C\hat{}N\hat{}N)_2Pt_2(\mu\text{-dppm})]^{2+}$[a,b]	3.245	20.7	–
$[((4\text{-}ClC_6H_4)\text{-}C\hat{}N\hat{}N)_2Pt_2(\mu\text{-dppm})]^{2+}$[a,b]	3.150	27.2	–
2a[b]	3.165	16.3	–
2b[b]	3.198	29.7	–
2c[b]	3.374	1.8	–
2d[b]	3.294	0.2	–
2f[b]	3.276	0.2	–
5b	3.300, 3.533	8.9, 29.3	163
$[(C\hat{}N\hat{}N)_3Pt_3(\mu\text{-dpmp})]^{3+}$[a]	3.194, 3.399; 3.364, 3.617	15.5, 26.3; 4.7, 34.6	162
$[(t\text{Bu}C\hat{}N\hat{}N)_3Pt_3(\mu\text{-dpmp})]^{3+}$[a]	3.217, 3.601	9.3, 29.6	157
$[(EtO_2CC\hat{}N\hat{}N)_3Pt_3(\mu\text{-dpmp})]^{3+}$[a]	3.466, 3.647	8.9, 33.7	162

[a] See references [13], [16], [18], and [20]. [b] In *syn*-form.

angles of 29.3° and 8.9°, respectively, and estimated interplane distances of about 3.3–3.5 Å; these structural data resemble those in the trinuclear (C^N^N) analogues (5–35° and 3.2–3.7 Å).[16] The Pt···Pt distances and torsion angles for the dinuclear and trinuclear complexes are listed in Table 4. The displaced (RC^N^N)Pt planes in **5b** are no longer parallel as in the dinuclear analogue **2b**, presumably due to the bulkiness of the *tert*-butyl group on the (RC^N^N) ligand.

In previous work on the [(C^N^N)PtX] system,[13,16,18,20] shorter Pt···Pt distances are accompanied by a larger torsion angle between the two (C^N^N)Pt moieties. This was attributed to a repulsive effect between the (C^N^N) ligands in a staggered rather than an eclipsed conformation.[35] In this work, the extended π-conjugation in (RC^N^N) leads to increased intramolecular metal–metal and ligand–ligand interactions in the dinuclear $[(RC\hat{}N\hat{}N)_2Pt_2(\mu\text{-dppm})](ClO_4)_2$ complexes. Such intramolecular interactions restrict the molecular motion of the flexible Pt-P-CH_2-P-Pt moiety and could be the reason for the enhancement of the corresponding emission intensity in solution, as discussed in the following section.

Absorption and emission spectroscopy of the mononuclear complexes: The spectroscopic and photophysical data of **1a**–**1f**, **3c**, **4b**, **4c**, **5b** and **5d** are listed in Table 5. The absorption spectra of **1a**–**1f**, **3c**, **4b** and **4c** reveal several intense transitions at λ_{max} values ranging from 250–390 nm. These were assigned to be mainly due to intraligand transitions since similar absorptions are found in the free (RC^N^NH) ligand.

The broad absorption at 400–470 nm ($\varepsilon \approx 6800$–$10000\ cm^{-1}mol^{-1}dm^3$) for **1a**–**1f** could be attributed to a ^{1}MLCT (5d)Pt→π*(L) transition, although mixing with IL could not be excluded. The absorption tail at around 500 nm is tentatively assigned to a ^{3}MLCT transition.[11,13,16,18,20,36,38,39] The absorption spectra of **1d** in CH_2Cl_2 and DMF solution are depicted in Figure 6 as an example. The absorption band at around 450 nm exhibits only a small solvatochromic shift (8 nm) on changing from CH_2Cl_2 to DMF.

Complexes **1a**–**1f** [(RC^N^N)PtCl] are strongly emissive, with λ_{max} that depend on the substituent group R. The emission energy in solution follows the order: R = 3,5-(tBu)$_2$Ph (**1d**, λ_{max} = 533 nm) > phenyl (**1c**, 537) in CH_2Cl_2 (2×10^{-5} M), and 3,5-F_2Ph (**1e**, 614) > 3,5-$(CF_3)_2$Ph (**1f**, 618) in DMF (2×10^{-5} M). A similar trend has also been observed for the emission of the $[(RC\hat{}N\hat{}N)Pt(PCy_3)]^+$ complexes **4b** and **4c** in MeCN (8×10^{-5} M): R = phenyl (**4c**, 621 nm) < tBu (**4b**, 603). The emission spectra recorded for **1e** and **1f** in DMF solution are not vibronically resolved. We assigned the emission of **1a**–**1f**, **3b**, **4b** and **4c** at 525–618 nm (CH_2Cl_2, MeCN or DMF solution) to a triplet excited state with ^{3}IL and ^{3}MLCT parentage. There is a lack of dependence of the

Table 5. Spectroscopic and photophysical data for **1a**–**1f**, **3c**, **4b**, and **4c**.

	Medium (T [K])	λ_{abs} [nm][a,b] (ε [$\times10^4$ cm^{-1}mol^{-1}dm^3])	λ_{em} [nm][c] (τ [μs]); k_q [10^9 s^{-1}dm^{-1}mol^{-1}][e]	Φ_{em}[d]
1a	CH_2Cl_2 (298)	249 (6.29), 289 (3.84), 307 (4.36), 343 (3.37), 381 (1.12), 416 (0.48), 451 (0.18), 500 (~0.01)	529 (6), 566, 595[f]; 6.8	0.20
	solid (298)	–	588 (6), 635 (6), 694 (6)	–
	solid (77)	–	588 (14), 639 (14), 699 (14)	–
	2-MeTHF (77)	–	521 (88), 563 (88), 609 (88)[b]	–
1b	CH_2Cl_2 (298)	250 (5.01), 290 (3.54), 305 (3.46), 342 (2.68), 375 (0.92), 408 (0.44), 450 (0.11), 500 (~0.01)	525 (6), 566, 591 (6), 633, 703[f]; 0.8	0.29
	solid (298)	–	609 (1), 693 (1)	–
	solid (77)	–	578 (13), 593 (13), 626 (13)	–
	2-MeTHF (77)	–	518 (97), 567 (97), 576 (32), 624 (32)[b]	–
1c	CH_2Cl_2 (298)	260 (6.40), 313 (4.69), 344 (3.04), 387 (0.99), 417 (0.60), 454 (0.10), 500 (~0.02)	537 (7), 570[f]; 9.0	0.42
	solid (298)	–	615 (5)	–
	solid (77)	–	603 (9), 654 (9)	–
	2-MeTHF (77)	–	525 (43), 567 (43), 614 (43)[b]	–
1d	CH_2Cl_2 (298)	254 (6.43), 314 (5.05), 344 (3.30), 386 (1.07), 415 (0.68), 458 (0.12), 500 (~0.01)	533 (7), 569[f]; 1.6	0.68
	DMF (298)	351 (4.84), 324 (4.89), 386 (1.22), 416 (0.78), 450 (0.22)	601 (11)[f]; 0.5	0.02
	solid (298)	–	613 (2), 659 (2)	–
	solid (77)	–	610 (11), 659 (11), 720 (11)	–
	2-MeTHF (77)	–	523 (52), 566 (52), 617 (52)[b]	–
1e	DMF (298)	315 (4.19), 343 (2.88), 395 (1.09), 422 (0.64), 465 (0.11), 500 (~0.01)	614 (0.7)[f]; 1.2	0.03
	solid (298)	–	615 (3), 661 (3), 725 (3)	–
	solid (77)	–	615 (10), 668 (10), 728 (10)	–
	2-MeTHF (77)	–	532 (33), 575 (33), 619 (33)[b]	–
1f	DMF (298)	316 (4.41), 344 (3.03), 395 (1.19), 427 (0.61), 467 (0.10), 500 (~0.04)	618 (0.7)[f]; 0.9	0.02
	solid (298)	–	626 (2)	–
	solid (77)	–	618 (12), 669 (12)	–
	DMF/MeOH/EtOH (1:1:4) (77)	–	537 (35), 596 (35), 650 (35), 715 (35)[b]	–
3c	MeCN (298)	196 (13.2), 247 (6.8), 310 (5.8), 388 (1.4), 500 (~0.05)	520 (8), 560 (8), 612 (8)[b]; 2.1	0.02
	solid (298)	–	599 (15), 650 (15), 707 (15)	–
	solid (77)	–	595 (35), 651 (35), 713 (35)	–
	DMF/MeOH/EtOH (1:1:4) (77)	–	516 (830), 558 (830), 605 (830)	–
4b	MeCN (298)	242 (5.4), 281 (4.0), 315 (4.0), 378 (1.2), 500 (~0.03)	603 (3)[b]; 2.5	0.08
	solid (298)	–	611 (11)	–
	solid (77)	–	603 (43), 640 (43), 702 (43)	–
	DMF/MeOH/EtOH (1:1:4) (77)	–	515 (880), 555 (880), 606 (880)	–
4c	MeCN (298)	250 (6.9), 313 (5.3), 389 (1.3), 500 (~0.01)	521, 561, 611 (3.0)[b]; 2.2	0.003
	solid (298)	–	633 (17)	–
	solid (77)	–	620 (74), 673 (74)	–
	DMF/MeOH/EtOH (1:1:4) (77)	–	521 (540), 564 (540), 611 (540)	–

[a] Absorption maxima. [b] At 4×10^{-5} M. [c] Emission maxima. [d] Emission quantum yield. [e] Emission self-quenching constant. [f] At 2×10^{-5} M.

emission energies on the complex concentrations from 10^{-4} to 10^{-6} M, which suggests that these emissions are not excimeric $^3\pi$–π^* or ^{3}MMLCT in nature; these emissions are probably ^{3}IL charge-transfer in nature. The emission of **1d** is affected by the solvent: its λ_{max} red-shifts from 533 nm in CH_2Cl_2 to 601 nm in DMF solution (Figure 6).

The emission quantum yields of **1a**–**1d** in CH_2Cl_2 solution range from 0.20 to 0.68, which are significantly higher than that of the congeners [(C^N^N)PtCl] ((C^N^N) = 6-phenyl-2,2′-bipyridyl and derivatives; $\Phi\approx0.03$–0.07).[13,20] It is likely that the extended π-conjugated (RC^N^N) ligands have a rigid structure, which disfavors deactivation of the excited state by (a) non-radiative process(es). The emission quantum yields of **1e** and **1f** in DMF are 0.02–0.03, lower than that of **1a**–**1d** in CH_2Cl_2 solution, probably due to the quenching effect of DMF. When the auxiliary Cl ligand is replaced with PPh_3 or PCy_3, as in **3c**, **4b** and **4c**, the quantum yield (0.003–0.08) decreases significantly.

In the solid state at room temperature, **1a**–**1f**, **3b**, **4b** and **4c** show a vibronic structured emission with λ_{max} at 588–633 nm. Upon cooling to 77 K, the emission is slightly blue-shifted. These emissions are assigned to ^{3}MLCT excited states. Glassy solutions (2-MeTHF or DMF/MeOH/EtOH, 1:1:4, 4×10^{-5} M) of **1a**–**1f**, **3b**, **4b** and **4c** were found to ex-

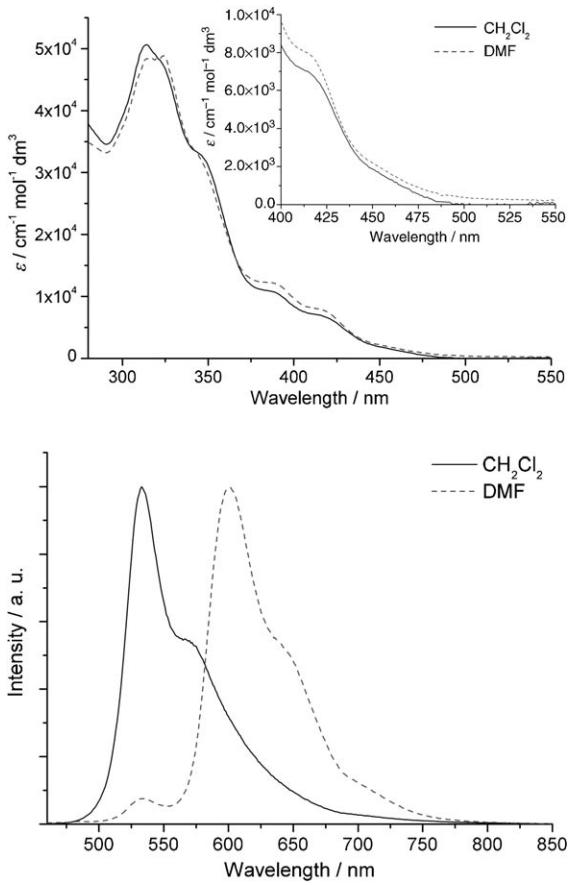

Figure 6. Absorption (top) and emission (bottom) spectra of **1d** in CH_2Cl_2 and DMF solution. Inset: expanded spectra in the region of 400 to 550 nm.

hibit similar vibronically structured emissions, with peak maxima at 518–537 nm. The spacings are 1300–1400 cm^{-1}, which correspond to the skeletal vibrational frequencies of the C=C/C=N entities of the (RC^N^N) ligands.[13,16,18,20]

Absorption and emission spectroscopy of the dinuclear and trinuclear complexes: Spectroscopic and photophysical data of **2a–2f**, **5b** and **5d** are listed in Table 6. Dinuclear complexes **2a–2f** show intense absorptions at around 390 nm ($\varepsilon \sim 2\times10^4\ cm^{-1}mol^{-1}dm^3$), with tailing from around 420 to 525 nm ($\varepsilon \sim 0.2\times10^4\ cm^{-1}mol^{-1}dm^3$), while the trinuclear complexes **5b** and **5d** show intense absorptions band at around 400 nm ($\varepsilon \sim 2\times10^4\ cm^{-1}mol^{-1}dm^3$), with tailing from around 450 to 550 nm ($\varepsilon \sim 0.25\times10^4\ cm^{-1}mol^{-1}dm^3$) in MeCN. Their mononuclear congeners [(RC^N^N)PtCl] (**1a–1f**) have lower ε values in the spectral region around 475 nm. Previous works have shown that metal–metal and ligand–ligand interactions are present in these dinuclear Pt^{II} complexes, with intramolecular distances of 2.998–3.432 Å;[13,16–18,20,38,39] such interactions, according to Miskowski and Houlding, destabilize the d_σ* orbital and stabilize the lowest unoccupied $\sigma^*(\pi)$ level, resulting in a red-shifted $d_\sigma^* \rightarrow \sigma^*(\pi)$ transition.[8,40] Therefore, the low-energy absorptions at 420–525 nm for the dinuclear complexes and those at 450–550 nm for the trinuclear complexes are tentatively assigned to excited states with mixed MMLCT $^1[d_\sigma^* \rightarrow \sigma(\pi^*)]$ and IL $^1[\sigma^*(\pi) \rightarrow \sigma(\pi^*)]$ parentage. A ^{1}MMLCT transition has previously been reported in $[Pt_2(tpy)_2(Gua)]^{3+}$ (tpy = 2,2′:6′,2″-terpyridine, Gua = guanidine anion),[9] $[Pt_2(tpy)_2(\mu\text{-}pz)]^{3+}$ (pz = pyrazole)[17,39] and the 6-phenyl-2,2′-bipyridyl congener $[(C^N^N)_2Pt_2(\mu\text{-}dppm)]^{2+}$.[13,16,18,20] All of the absorption bands described above obey Beer's Law in the concentration range 10^{-3} to 10^{-6} M, thereby suggesting that there is no dimerization or oligomerization of the metal complexes in the ground state. Complex **2d** shows similar absorption profiles in MeCN, CH_2Cl_2, MeOH and DMF at room temperature; for example, the absorption band at about 470 nm exhibits only a small solvatochromic shift (±5 nm) upon changing the solvent from MeCN to CH_2Cl_2, MeOH and DMF (Figure 7). The absorption band of **5d** at about 500 nm in MeCN, CH_2Cl_2, MeOH and DMF at room temperature exhibits a similarly small solvatochromic shift (±5 nm; Figure 8).

Complexes **2a–2f** exhibit a peak maxima at 585–638 nm (Φ = 0.07–0.35) in acetonitrile at room temperature. The emission energy is affected by the substituent R on the (RC^N^N) ligand, and follows the order *t*Bu (**2b**, λ_{max} = 585 nm) > H (**2a**, 605) > 3,5-*t*Bu_2Ph (**2d**, 609) > phenyl (**2c**, 614) > 3,5-F_2Ph (**2e**, 637) ~3,5-$(CF_3)_2$Ph (**2f**, 638). Complexes **5b** and **5d** are strongly emissive in acetonitrile, with λ_{max} at 626 (Φ = 0.33) and 608 nm (Φ = 0.19), respectively. In conjunction with the observed intramolecular Pt···Pt contacts in the crystal structures of **2a**, **2c**, **2d**, **2f** and **5b**, the low-energy emission bands of the dinuclear and trinuclear complexes are assigned to a ^{3}MMLCT $^3[d_\sigma^* \rightarrow \sigma(\pi^*)]$ excited-state and are red-shifted in energy from that of their mononuclear congeners **1a–1d** and **1f** (λ_{max} = 529, 525, 537, 533 and 618 nm, respectively). The latter emissions come from a ^{3}MLCT excited state. At room temperature, the emissions of **2d** in MeCN, CH_2Cl_2, MeOH and DMF solution are similar in energy; their λ_{max} undergo only a small solvatochromic shift (±6 nm; Figure 7). However, the emission quantum yield of **2d** is strongly affected by the solvent (Φ = 0.26 in MeCN or CH_2Cl_2, 0.05 in MeOH and 0.08 in DMF; Figure 7), presumably due to a quenching effect in MeOH and DMF. While the emission quantum yield of **5d** is affected by solvent (Φ = 0.19 in MeCN, 0.29 in CH_2Cl_2, 0.04 in MeOH and < 0.01 in DMF), the λ_{max} shows only a small solvatochromic shift (±6 nm) when the solvent is changed from MeCN to CH_2Cl_2, MeOH and DMF (Figure 8).

Complexes **2a–2f** in the solid state at room temperature show λ_{max} at 585–636 nm, which are blue-shifted to 569–613 nm, upon cooling the samples to 77 K. In glassy solution (DMF/MeOH/EtOH, 1:1:4, 4×10^{-5} M), the emission is broad and intense, with λ_{max} ranging from 522 nm for **2d** to 605 nm for **2c**. The lack of vibronic structure and the concentration dependence suggest that the emission is unlikely to be ^{3}IL or excimeric $^3\pi$–π^*. These emissions are probably ^{3}MLCT in nature. Complexes **5b** and **5d** in the solid state at room temperature show λ_{max} at 623 and 618 nm, respectively, which blue shift to 603 and 605 nm, respectively, upon cooling the

Table 6. Spectroscopic and photophysical data for **2a**–**2f**, **5b**, and **5d**.

	Medium (T [K])	λ_{abs} [nm][a,b] (ε [$\times 10^4$ cm^{-1} mol^{-1} dm^3])	λ_{em} [nm][c,d] (τ [μs])	Φ_{em}[e]
2a	MeCN (298)	237 (11.69), 305 (5.59), 392 (1.84), 476 (0.17), 500 (~0.07)	605 (1)[f]	0.27
	solid (298)	–	636 (6)	–
	solid (77)	–	597 (1)	–
	DMF/MeOH/EtOH (1:1:4) (77)	–	601 (253)[g]	–
2b	MeCN (298)	230 (11.69), 308 (5.36), 378 (1.65), 408 (1.50), 450 (0.52), 500 (0.20)	585 (2)[f]	0.35
	solid (298)	–	617 (101)	–
	solid (77)	–	613 (20), 665 (20)	–
	DMF/MeOH/EtOH (1:1:4) (77)	–	525 (240), 574 (240)[g]	–
2c	MeCN (298)	242 (9.80), 306 (7.02), 391 (1.50), 464 (0.19), 500 (~0.08)	614 (2)[f]	0.32
	solid (298)	–	621 (4)	–
	solid (77)	–	569 (11), 611 (11), 668 (11)	–
	DMF/MeOH/EtOH, 1:1:4 (77)	–	605 (152)[g]	–
2d	MeCN (298)	240 (11.69), 312 (8.05), 384 (2.14), 466 (0.40), 500 (0.19)	609 (3)[f]	0.26
	CH_2Cl_2 (298)	325 (11.0), 383 (3.45), 450 (0.48), 500 (0.19)	606 (3)[f]	0.26
	MeOH (298)	205 (14.8), 322 (8.8), 383 (2.5), 450 (0.33)	618 (13)[f]	0.05
	DMF (298)	323 (9.57), 381 (2.74), 415 (1.18), 475 (0.25), 500 (0.14)	603 (11)[f]	0.08
	solid (298)	–	585 (13)	–
	solid (77)	–	595 (59)	–
	DMF/MeOH/EtOH (1:1:4) (77)	–	522 (205), 564 (205)[g]	–
2e	MeCN (298)	242 (12.41), 294 (8.76), 395 (2.18), 474 (0.51), 500 (0.33), 525 (0.17)	637 (0.2)[f]	0.07
	solid (298)	–	600 (4), 635 (4)	–
	solid (77)	–	597 (7)	–
	DMF/MeOH/EtOH (1:1:4) (77)	–	618 (125)[g]	–
2f	MeCN (298)	256 (11.59), 302 (7.25), 386 (2.05), 476 (0.17), 500 (~0.08)	638 (0.2)[f]	0.09
	solid (298)	–	613 (2)	–
	solid (77)	–	609 (3)	–
	DMF/MeOH/EtOH (1:1:4) (77)	–	598 (103)	–
5b	MeCN (298)	237 (15.9), 303 (7.8), 400 (2.4), 475 (0.44), 500 (~0.22)	626 (2.4)[f]	0.33
	solid (298)	–	623 (1.6)[f]	–
	solid (77)	–	603 (1.6)[f]	–
	DMF/MeOH/EtOH (1:1:4) (77)	–	530 (220), 577 (220)[g]	–
5d	MeCN (298)	238 (15.7), 314 (10.5), 400 (2.3), 450 (0.51), 500 (0.34)	608 (1.7)[f]	0.19
	CH_2Cl_2 (298)	238 (18.3), 315 (12.3), 391 (3.1), 410 (2.8), 475 (0.4), 500 (0.25)	606 (1.7)[f]	0.29
	MeOH (298)	205 (18.1); 240 (16.1), 314 (12.1), 404 (2.8), 475 (0.51), 500 (0.26)	601 (10)[f]	0.04
	DMF (298)	314 (12.6), 395 (3.0), 411 (2.9), 500 (0.29)	607 (11)[f]	<0.01
	solid (298)	–	618 (1.2)	–
	solid (77)	–	605 (4.6)	–
	DMF/MeOH/EtOH (1:1:4) (77)	–	519 (770), 563(770)[g]	–

[a] Absorption maxima. [b] At 1×10^{-5} M. [c] Emission maxima. [d] Self-quenching of emission is not observed. [e] Emission quantum yield. [f] At 2×10^{-5} M. [g] At 4×10^{-5} M.

samples to 77 K. In glassy solution (DMF/MeOH/EtOH, 1:1:4, 4×10^{-5} M), the emission is vibronically structured with peak maxima at 519–577 nm. The spacings of 1300–1400 cm^{-1} correspond to the skeletal vibrational frequencies of the C=C/C=N entities of the (RC^N^N) ligands; therefore, we can assign these emissions as coming from a ^{3}IL excited state.

Excited state reduction potential: The excited state reduction potential ($E_{1/2}$*), defined by $Pt_n^* + e^- \rightarrow [Pt_n]^-$ ($n=1$, 2, 3), of $[(RC^N^N)PtX](ClO_4)_n$, $[(RC^N^N)_2Pt_2(\mu\text{-dppm})](ClO_4)_2$ and $[(RC^N^N)_3Pt_3(\mu\text{-dpmp})](ClO_4)_3]$ were estimated from the electrochemical and spectroscopic data using the equation $E_{1/2}^* = E_{1/2} + E_{0\text{–}0}$,[6,16] and compared to the values for [4,4′-tBu$_2$(C^N^N)Pt(PPh$_3$)](ClO$_4$), [4-EtO$_2$C-(C^N^N)Pt(PPh$_3$)](ClO$_4$), [4,4′-tBu$_2$(C^N^N)$_2$Pt$_2$(dppm)](ClO$_4$)$_2$, [{4-EtO$_2$C(C^N^N)}$_2$Pt$_2$(dppm)](ClO$_4$)$_2$ and $[(C^N^N)_2Pt_2(dppm)]^{2+}$.[6,16] $E_{1/2}$ values from the first reversible reduction wave were used in these calculations. The $E_{0\text{–}0}$ transitions were estimated from the emission maxima of the complexes in alcoholic glassy solution at 77 K. These calculations ignore the differences between $E_{0\text{–}0}$ and the emission maxima, in addition to any effect from employing different solvents in electrochemical and spectroscopic measurements; we are only interested in the relative trend in the excited state reduction potential of these complexes. The $E_{1/2}$* values for those complexes with an auxiliary Cl ligand (**1a**–**1f**), found at 0.5–0.6 V versus $Cp_2Fe^{+/0}$, are the lowest among the Pt^{II}(R C^N^N) complexes studied in this work. These values are smaller than those calculated for the mononuclear and dinuclear 6-phenyl-2,2′-bipyridyl (C^N^N) congeners (0.9–1.4 V).[13,15,16] The other mononuclear complexes with PPh_3 and PCy_3 (**3c**, **4b** and **4c**) have $E_{1/2}$* values of 0.8–0.9 V. Of the dinuclear complexes, **2a** and **2c** have low $E_{1/2}$* values (0.6 V), while **2b**, **2d**, **2e** and **2f** have higher values of between 0.7 and 0.9 V versus $Cp_2Fe^{+/0}$. The $E_{1/2}$* values of the trinuclear complexes **5b** and **5d** are 0.7 and 0.9 V versus $Cp_2Fe^{+/0}$, respectively.

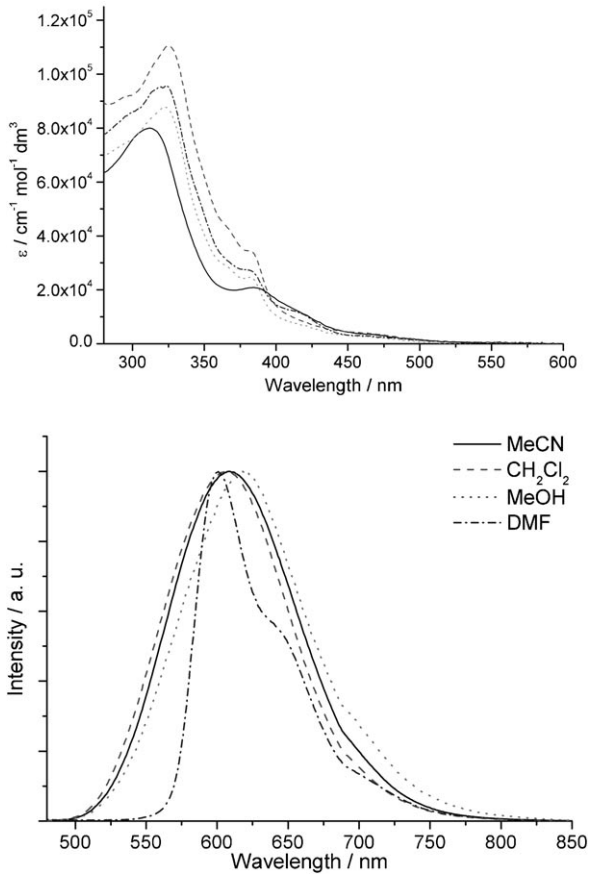

Figure 7. Absorption (top) and emission (bottom) spectra of **2d** in MeCN, CH_2Cl_2, MeOH and DMF solution.

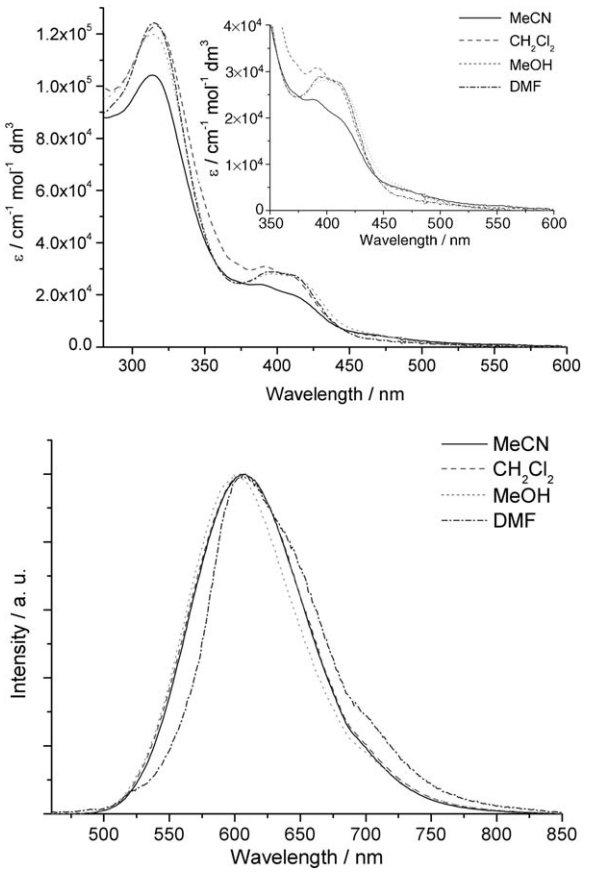

Figure 8. Absorption (top) and emission (bottom) spectra of **5d** in MeCN, CH_2Cl_2, MeOH and DMF solution. Inset: expanded ε values versus wavelength plots in the 350 to 600 nm region.

Electroluminescence of 1a and 1d: The [(RC^N^N)PtCl] complexes possess high PL quantum yields and thermal stabilities yet they can be easily sublimed in vacuo. These properties render them suitable for applications in OLEDs. The OLEDs in this work were fabricated with 1–6% of **1a** or **1d** as the emitting dopant. The devices containing **1a** have the following configuration: ITO (indium tin oxide)/NPB (4,4′-bis[*N*-(1-naphthyl)-*N*-phenylamino]biphenyl 70 nm)/CBP (4,4′-*N*,*N*′-dicarbazolebiphenyl):**1a** (x%, 30 nm)/BCP (bathocuprine, 15 nm)/Alq_3 (tris(8-quinolinolato)aluminium, 30 nm)/LiF (0.3 nm)/Al (130 nm). A data summary for these devices is depicted in Table 7. A dopant concentration of 5% (device **A**) gave the best performance. This device is a yellow-green light emitter; a strong emission was observed with peak maxima at 532 and 570 nm and a shoulder at about 610 nm, which could be attributed to the triplet excited state of **1a**. A brightness of 1 cd m^{-2} was obtained at 5 V. The maximum brightness of 37400 cd m^{-2} was achieved at 20 V, and the maximum current efficiency of 15.4 cd A^{-1} was reached at 0.2 mA cm^{-2}.

Table 7. EL data for **1a** and **1d**.

Device[a]	Complex	x[b] [%]	B_{max} [cd m^{-2}] (V [V])[c]	CIE[d] x, y	Eff_{max} [cd A^{-1}] (J [mA cm^{-2}])[e]
A	**1a**	5	37000 (20)	0.37, 0.58	15.4 (0.2)
B	**1d**	1	63000 (20)	0.36, 0.54	12.5 (1.7)
C	**1d**	3	40000 (21)	0.38, 0.55	20.2 (0.4)

[a] Devices **A**, **B**, and **C** gave a brightness of 1 cd m^{-2} at 5 V. [b] Dopant percentage of **1a** or **1d**. [c] Maximum brightness (B_{max}) achieved at voltage V. [d] 1931 Commission Internationale de l'Éclairage coordinates at achieved maximum brightness. [e] Maximum current efficiency (Eff_{max}) achieved at current density J.

OLEDs employing **1d** (1–12%) were prepared in the following configuration: ITO/NPB (40 nm)/CBP:**1d** (x%, 30 nm)/$BAlq_3$ (bis(2-methyl-8-quinolinolato)(4-phenylphenolato)aluminum, 10 nm)/Alq_3 (30 nm)/LiF (0.1 nm)/Al (200 nm). Devices **B** (x=1%) and **C** (x=3%) gave the highest maximum brightness and current efficiency, respectively (Table 7). These devices are also yellowish-green light emitters and have similar CIE coordinates (Table 7). The EL λ_{max} (540 and 592 nm, with a shoulder at about 640 nm) is independent of the doping concentration for **1d**. The good performance of these devices can be correlated to the high emission quantum yield, T_d, and T_g of **1d**. Device B gave a brightness of 1 cd m^{-2} at 5 V, and a maximum current efficiency of 12.5 cd A^{-1} was obtained at 1.8 mA cm^{-2}. This device is stable in terms of efficiency decay, and the efficiency was attained at 5 cd A^{-1} when the current density was in-

creased to 600 mA cm^{-2}. A maximum brightness of 63000 cd m^{-2} was achieved at 20 V (Figure 9); this is significantly higher than those yellow to yellowish-green OLEDs employing the 6-phenyl-2,2′-bipyridyl congener $[(C^N^N)PtR]^+$ (maximum luminance = 7800 cd m^{-2}, λ_{max} =

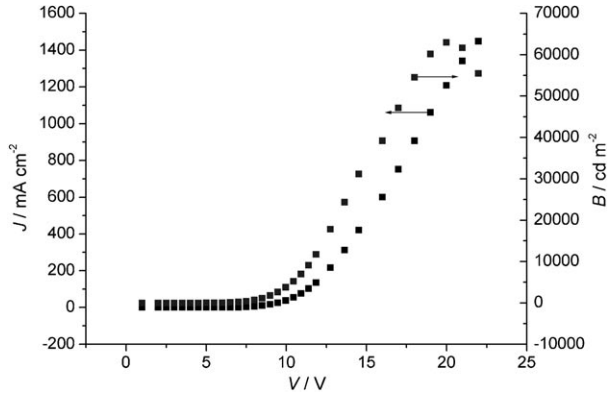

Figure 9. *J–V–B* (current density–voltage–brightness) relationships of device **B**.

564 nm),[15] $[Pt(N_2O_2)]$ (4480 cd m^{-2}; CIE $x = 0.42$, $y = 0.56$),[33] Pt Schiff-base complexes (23000 cd m^{-2}; CIE $x = 0.48$, $y = 0.52$),[41] [(O^N^N)PtCl] ((O^N^N) = derivatives of 6-(2-hydroxyphenyl)-2,2′-bipyridyl; maximum luminance = 37000 cd m^{-2}, CIE $x = 0.48$, $y = 0.51$),[32] [(X-bt)Pt(acac)] (11320 cd m^{-2} at 14 V; CIE $x = 0.47$, $y = 0.51$; X-bt = substituted 2-phenylbenzothiazolato (X = H or F); acac = acetylacetonate),[42] $[Pt(N^N)_2]$ ((N^N) = 5-(2-pyridyl)-3-trifluoromethylpyrazole; maximum luminance = 41000 cd m^{-2}, CIE $x = 0.42$, $y = 0.53$; Table 8)[43] and other non-Pt emitters as dopants.[44–46]

Conclusions

In the past few years there has been an increasing interest in luminescent platinum(II) complexes, especially those with diimine and cyclometalated ligands, due to their possible application as phosphorescent materials for organic light-emitting devices.[15,16,19,32,33,41,43,47–53] The mono-, di- and trinuclear (RC^N^N) complexes of platinum(II) reported in this work are strongly emissive and have high emission quantum yields in solutions at room temperature. The emission quantum yield of **1d** (0.68 in CH_2Cl_2) is significantly higher than that of $[(C^N^N)PtCl]$[13] and $[Pt(tBu_2N_2O_2)]$,[32] with the latter two showing emission at 565 ($\Phi = 0.025$) and 595 nm ($\Phi = 0.12$), respectively, in CH_2Cl_2 solutions (Table 8). The ^{3}MMLCT excited states of $[(RC^N^N)_2Pt_2(\mu\text{-dppm})](ClO_4)_2$ (**2b**) and $[(RC^N^N)_3Pt_3(\mu\text{-dpmp})](ClO_4)_3$ (**5b**) have a high emission quantum yield (0.35 for **2b** and 0.33 for **5b**) in solution at room temperature, and this is quite uncommon for di- and trinuclear platinum(II) complexes. There are several unique features of the (RC^N^N) ligands that may account for the high emission quantum yields of their Pt^{II} complexes: 1) the extended π-conjugation would increase the electronic delocalization, hence a smaller bond displacement change in the excited state compared to those for (C^N^N) analogues is expected. This would lead to less effective non-radiative decay;[54] 2) the rigid planar geometry of the (RC^N^N) ligands maintains the stereochemical integrity of the mononuclear complexes, and the extensive inter- and/or intramolecular π···π interactions reduce molecular motions, particularly at the flexible Pt-P-CH_2-P-Pt moiety in the binuclear complexes, and discourage excited state distortions, thereby reducing non-radiative decay. The mononuclear Cl-containing complexes **1a** and **1c** have an almost planar geometry that enables close intermolecular interplanar contacts. The dinuclear complexes **2c**, **2d** and **2f** exhibit an eclipsed overlap of

Table 8. Comparison of the properties of the platinum(II) light-emitting materials.

Complex	λ_{maxPL}[a] [nm]	Φ_{em}[b]	OLED Device Performance					
			T_d[c] [°C]	λ_{maxEL}[d] [nm]	CIE[e] x, y	x[f] [%]	B_{max} [cd m^{-2}] (V [V])[g]	Eff_{max} [cd A^{-1}] (J [mA cm^{-2}])[h]
1a	529 (CH_2Cl_2)	0.20 (CH_2Cl_2)	470	532, 570	0.37, 0.58	5	37000 (20)	15.4 (0.2)
1d	533 (CH_2Cl_2)	0.68 (CH_2Cl_2)	532	540, 592	0.38, 0.55	1	63000 (20)	12.5 (1.7)
$[(C^N^N)PtCl]$[i]	565 (CH_2Cl_2)	0.025 (CH_2Cl_2)	285	–	–	–	–	–
$[(C^N^N)PtC{\equiv}CC_6H_5]$[j]	582 (CH_2Cl_2)	0.04 (CH_2Cl_2)	~400	564	0.48, 0.48	4	7800 (11)	2.4 (30)
$[(C^N^N)PtC{\equiv}CC_6F_5]$[j]	560 (CH_2Cl_2)	0.06 (CH_2Cl_2)	~400	548	0.44, 0.51	4	9800 (12)	3.2 (20)
$[(S^N^N)PtC{\equiv}CC_6H_4\text{-}4\text{-}CH_3]$[j]	616 (CH_2Cl_2)	0.04 (CH_2Cl_2)	~400	612	0.59, 0.34	4	3100 (12)	1.0 (30)
$[(O^N^N)PtCl]$[k]	606 (DMF)	0.01 (DMF)	388	564	0.48, 0.50	6	6000 (16)	2.9 (4.4)
$[(O^N^N)PtCl]$[k]	600 (DMF)	0.02 (DMF)	421	565	0.51, 0.48	5	14000 (16)	9.7 (4.2)
$[(O^N^N)PtCl]$[k]	593 (DMF)	0.03 (DMF)	425	564	0.50, 0.49	6	26000 (14)	13 (1.4)
$[(O^N^N)PtCl]$[k]	618 (DMF)	0.01 (DMF)	351	572	0.53, 0.46	6	10000 (19)	7.3 (2.9)
$[(O^N^N)PtCl]$[k]	606 (DMF)	0.04 (DMF)	426	566	0.48, 0.51	5	37000 (16)	7.8 (89)
$[Pt(tBu_2N_2O_2)]$[l]	595 (CH_2Cl_2)	0.12 (CH_2Cl_2)	530	540	–	0.3	9330 (–)	–
[(x-bt)Pt(acac)][m]	531, 571 (CH_2Cl_2)	–	–	–	0.47, 0.51	5	11320 (14)	16 (2)
$[Pt(N^N)_2]$[n]	595 (solid state)	0.24 (solid state)	–	560	0.42, 0.53	20	41000 (15)	20 (20)

[a] Peak maximum of photoluminescence. [b] Emission quantum yield in solution. [c] Decomposition temperature. [d] Peak maximum of electroluminescence. [e] 1931 Commission Internationale de l'Éclairage coordinates. [f] Dopant percentage of platinum(II) complex. [g] Maximum brightness (B_{max}) achieved at voltage V. [h] Maximum current efficiency (Eff_{max}) achieved at current density J. [i] Reference [13]. [j] Reference [15]. [k] Reference [32]. [l] Reference [33]. [m] Reference [42]. [n] Reference [43].

the (RC^N^N) moieties with torsion angles close to 0°. In previous reports on [Pt(C^N^N)] systems, shorter Pt···Pt distances are accompanied by a larger torsion angle between the two (C^N^N)Pt moieties. This was attributed to a minimal repulsive effect between the (C^N^N) ligands in a staggered rather than an eclipsed conformation.[35] The extensive π···π interactions in $[(RC^N^N)_2Pt_2(\mu\text{-dppm})](ClO_4)_2$ are evident from the torsion angles in **2c**, **2d** and **2f** (1.8°, 0.2° and 0.2°, respectively), which are significantly smaller than that in $[(C^N^N)_2Pt_2(\mu\text{-dppm})]^{2+}$ (44.6°, Table 4). The [(RC^N^N)PtCl] complexes have been demonstrated to be useful phosphorescent materials. High-performance light-emitting devices have been fabricated from **1a** and **1d**; the performances of these yellow OLEDs are significantly better than those employing other platinum(II) complexes in terms of both luminance and efficiency. For example, the yellow OLED (EL $\lambda_{max}=536$ nm) containing **1d** as the emitter exhibits a maximum luminance of 63000 cd m^{-2} and a current efficiency of 12.5 cd A^{-1} at a current density of 1.8 mA cm^{-2}, which are higher than those obtained with [(O^N^N)PtCl] (566 nm, 37000 cd m^{-2} and 7.8 cd A^{-1} at 89 mA cm^{-2}, Table 8). The outstanding performance of these OLEDs can be related to the high emission quantum yields of [(RC^N^N)PtCl]. Due to the ease of modifying the chelating cyclometalated ligand, these complexes represent a new class of luminophores with tuneable excited-state properties. Along with their highly luminescent nature and appreciable thermal stability (with T_d up to around 530 °C for **1d**), cyclometalated (RC^N^N) systems of platinum(II) with extended π-conjugation constitute a new class of light-emitting materials with potential practical applications.

Experimental Section

General considerations: Solvents were purified according to literature methods.[55] 3-Acetylisoqulinoline was prepared from 3-hydroxyisoqulinoline by a Heck reaction.[56] 1-(2-(3′-Isoquinolinyl)-2-oxoethyl)pyridinium iodide was prepared by heating 3-acetylisoqulinoline with excess I_2 in pyridine for 2 h.[57–59] 3-Dimethylamino-1-(2′-naphthyl)propanone hydrochloride salt was synthesized by refluxing 2-acetylnaphthalene, paraformaldehyde and dimethylamine hydrochloride in the presence of conc. HCl in 95% ethanol for 24 h.[59] The α,β-unsaturated ketones were prepared according to literature methods.[60,61] The (RC^N^NH) ligands **a–f** were prepared by modification of published procedures.[62] Electron-impact (EI) and fast atom bombardment (FAB) mass spectra were obtained with a Finnigan Mat 95 mass spectrometer. ^{1}H and ^{31}P NMR spectra were recorded with Bruker AVANCE 600, DRX 400 and 500 FT-NMR spectrometers. The ^{1}H NMR chemical shifts were referenced to those of the residual proton/carbon atoms of CD_3CN, [D$_7$]DMF, $CDCl_3$ or CD_2Cl_2. H_3PO_4 was used in the ^{31}P NMR study as external reference. Peak assignments were based on results of ^{1}H–^{1}H and NOESY 2D NMR experiments. Elemental analyses were performed at the Institute of Chemistry of the Chinese Academy of Science in Beijing.

Synthesis of (RC^N^NH) (a–f)

General procedure: Heating a mixture of 1-(2-(3′-isoquinolinyl)-2-oxoethyl)pyridinium iodide, 3-dimethylamino-1-(2′-naphthyl)propanone hydrochloride salt (for **a**) or the corresponding α,β-unsaturated ketone (for **b–f**) and excess ammonium acetate in methanol (100 mL) for 24 h gave **a–f**. The crude product was filtered from the solution mixture, washed with water and cold methanol, and purified by column chromatography (silica gel, *n*-hexane/$CHCl_3$ = 9:1 as eluent). The structures and numbering schemes of **a–f** for NMR peak assignment are depicted in Figure 1.

(HC^N^NH) (a): 1-(2-(3′-Isoquinolinyl)-2-oxoethyl)pyridinium iodide (1.00 g, 2.66 mmol), 3-dimethylamino-1-(2′-naphthyl)propanone hydrochloride salt (0.70 g, 2.7 mmol) and ammonium acetate (5.00 g, 64.9 mmol) gave **a** as an off-white solid. Yield: 0.53 g (60%); ^{1}H NMR (300 MHz, $CDCl_3$, 25 °C, TMS): δ = 7.5–7.6 (m, 2H; H^6 and H^7), 7.7 (t, $^3J_{H,H}$ = 8 Hz, 1H; H^{21}), 7.8 (t, $^3J_{H,H}$ = 9 Hz, 1H; H^{20}), 7.9–8.1 (m, 7H; H^3, H^5, H^8, H^{12}, H^{13}, H^{19} and H^{22}), 8.4 (dd, $^4J_{H,H}$ = 2, $^3J_{H,H}$ = 10 Hz, 1H; H^2), 8.5 (dd, $^4J_{H,H}$ = 1, $^3J_{H,H}$ = 9 Hz, 1H; H^{14}), 8.7 (s, 1H; H^{10}), 9.1 (s, 1H; H^{24}), 9.4 ppm (s, 1H; H^{17}); MS (70 eV, EI): *m*/*z* 332 [*M*$^+$].

(*t*BuC^N^NH) (b): 1-(2-(3′-Isoquinolinyl)-2-oxoethyl)pyridinium iodide (0.47 g, 1.3 mmol), *tert*-butylidene-2-acetonaphthone (0.30 g, 1.3 mmol) and ammonium acetate (5.00 g, 64.9 mmol) gave **b** as an off-white solid. Yield: 0.27 g (55%); ^{1}H NMR (300 MHz, $CDCl_3$, 25 °C, TMS): δ = 1.5 (s, 9H; C(CH$_3$)$_3$), 7.3–7.6 (m, 2H; H^6 and H^7), 7.6 (t, $^3J_{H,H}$ = 8 Hz, 1H; H^{21}), 7.7 (t, $^3J_{H,H}$ = 8 Hz, 1H; H^{20}), 7.9 (m, 2H; H^5 and H^{12}), 8.0–8.1 (m, 4H; H^3, H^8, H^{19} and H^{22}), 8.4 (dd, $^4J_{H,H}$ = 2, $^3J_{H,H}$ = 5 Hz, 1H; H^2), 8.6 (d, $^4J_{H,H}$ = 1.6 Hz, 1H; H^{14}), 8.6 (s, 1H; H^{10}), 9.1 (s, 1H; H^{24}), 9.4 ppm (s, 1H; H^{17}); MS (70 eV, EI): *m*/*z* 388 [*M*$^+$].

(PhC^N^NH) (c): 1-(2-(3′-Isoquinolinyl)-2-oxoethyl)pyridinium iodide (1.00 g, 2.66 mmol), benzylidene-2-acetonaphthone (0.69 g, 2.7 mmol) and ammonium acetate (5.00 g, 64.9 mmol) gave **c** as a white solid. Yield: 0.87 g (80%); ^{1}H NMR (400 MHz, $CDCl_3$, 25 °C, TMS): δ = 7.5 (t, $^3J_{H,H}$ = 6 Hz, 1H; H^{28}), 7.5–7.6 (m, 4H; H^5, H^7 and H^{27}), 7.7 (t, $^3J_{H,H}$ = 8 Hz, 1H; H^{21}), 7.8 (t, $^3J_{H,H}$ = 8 Hz, 1H; H^{20}), 7.9–8.0 (m, 3H; H^8 and H^{26}), 8.0–8.1 (m, 4H; H^3, H^6, H^{19} and H^{22}), 8.1 (s, 1H; H^{12}), 8.5 (d, $^3J_{H,H}$ = 5 Hz, 1H; H^2), 8.7 (s, 1H; H^{10}), 8.8 (s, 1H; H^{14}), 9.1 (s, 1H; H^{24}), 9.4 ppm (s, 1H; H^{17}); MS (70 eV, EI): *m*/*z* 408 [*M*$^+$].

(3,5-*t*Bu$_2$PhC^N^NH) (d): 1-(2-(3′-Isoquinolinyl)-2-oxoethyl)pyridinium iodide (0.90 g, 2.4 mmol), 3′,5′-di-*tert*-butylbenzylidene-2-acetonaphthone (0.89 g, 2.4 mmol) and ammonium acetate (5.00 g, 64.9 mmol) gave **d** as a white solid. Yield: 0.89 g (72%); ^{1}H NMR (400 MHz, $CDCl_3$, 25 °C, TMS): δ = 1.5 (s, 18H; C(CH$_3$)$_3$), 7.6–7.7 (m, 6H; H^6, H^8, H^{21}, H^{26} and H^{28}), 7.8 (t, $^3J_{H,H}$ = 8 Hz, 1H; H^{20}), 7.9–8.0 (m, 1H; H^5), 8.0–8.1 (m, 5H; H^3, H^7, H^{12}, H^{19} and H^{22}), 8.5 (d, $^3J_{H,H}$ = 10 Hz, 1H; H^2), 8.7 (s, 1H; H^{10}), 8.8 (s, 1H; H^{14}), 9.1 (s, 1H; H^{24}), 9.4 ppm (s, 1H; H^{17}); MS (70 eV, EI): *m*/*z* 520 [*M*$^+$].

(3,5-F$_2$PhC^N^NH) (e): 1-(2-(3′-Isoquinolinyl)-2-oxoethyl)pyridinium iodide (1.91 g, 5.19 mmol), 3′,5′-difluorobenzylidene-2-acetonaphthone (1.53 g, 5.19 mmol) and ammonium acetate (5.00 g, 64.9 mmol) gave **e** as a white solid. Yield: 2.03 g (88.1%); ^{1}H NMR (400 MHz, CD_2Cl_2, 25 °C, TMS): δ = 7.0 (t, $^3J_{H,F}$ = 9 Hz, 1H; H^{28}), 7.4–7.5 (m, 2H; H^{26}), 7.6 (m, 2H; H^6 and H^8), 7.7 (t, $^3J_{H,H}$ = 8 Hz, 1H; H^{21}), 7.8 (t, $^3J_{H,H}$ = 8 Hz, 1H; H^{20}), 8.0 (m, 1H; H^5), 8.0–8.1 (m, 5H; H^3, H^7, H^{14}, H^{19} and H^{22}), 8.5 (d, $^3J_{H,H}$ = 10 Hz, 1H; H^2), 8.7 (s, 1H; H^{10}), 8.8 (s, 1H; H^{12}), 9.1 (s, 1H; H^{24}), 9.4 ppm (s, 1H; H^{17}); ^{19}F NMR (376 MHz, CD_2Cl_2, 25 °C): δ = −109.6 ppm (t, $^3J_{H,F}$ = 8 Hz); MS (70 eV, EI): *m*/*z* 444 [*M*$^+$].

(3,5-(CF$_3$)$_2$PhC^N^NH) (f): 1-(2-(3′-Isoquinolinyl)-2-oxoethyl)pyridinium iodide (0.95 g, 2.5 mmol), 3′,5′-bis(trifluoromethyl)benzylidene-2-acetonaphthone (1.00 g, 2.54 mmol) and ammonium acetate (5.00 g, 64.9 mmol) gave **f** as a white solid. Yield: 1.2 g (85%); ^{1}H NMR (400 MHz, $CDCl_3$, 25 °C, TMS): δ = 7.5–7.6 (m, 2H; H^6 and H^8), 7.7 (t, $^3J_{H,H}$ = 9 Hz, 1H; H^{21}), 7.8 (t, $^3J_{H,H}$ = 8 Hz, 1H; H^{20}), 7.9–8.0 (m, 1H; H^5), 8.0–8.1 (m, 6H; H^3, H^7, H^{12}, H^{19} and H^{22}), 8.3 (s, 2H; H^{26}), 8.4 (d, $^3J_{H,H}$ = 10 Hz, 1H; H^2), 8.7 (s, 1H; H^{10}), 8.8 (s, 1H; H^{14}), 9.1 (s, 1H; H^{24}), 9.4 ppm (s, 1H; H^{17}). ^{19}F NMR (376 MHz, 25 °C, TMS): δ = −62.6 ppm; MS (70 eV, EI): *m*/*z* 544 [*M*$^+$].

Synthesis of [(RC^N^N)PtCl] (1a–1f)

General procedure: Refluxing a mixture of K_2PtCl_4 and the corresponding (RC^N^NH) (**a–f**) in glacial acetic acid (100 mL) for 24 h gave **1a–1f** as a yellow suspension. The yellow solid was isolated by filtration, washed with water and acetone, and recrystallized from CH_2Cl_2 (for **1a**, **1c** and **1d**) or DMF (for **1b**, **1e** and **1f**). Complexes **1a–1f** are insoluble in most organic solvents; they are slightly soluble in [D$_7$]DMF but the solubility is too low to allow for ^{13}C NMR measurements. The structure

and numbering scheme of **1a–1f** for NMR peak assignment are depicted in Figure 1.

[(HC^N^N)PtCl] (1a): K_2PtCl_4 (0.22 g, 0.30 mmol) and **a** (0.10 g, 0.30 mmol) were used. Complex **1a** was isolated as a yellow, crystalline solid. Yield: 0.13 g (80%); ^{1}H NMR (400 MHz, [D$_7$]DMF, 25°C, TMS): δ=7.4 (t, $^3J_{H,H}$=7 Hz, 1H; H^6), 7.5 (t, $^3J_{H,H}$=7 Hz, 1H; H^7), 7.8 (d, $^3J_{H,H}$=9 Hz, 1H; H^8), 7.9 (d, $^3J_{H,H}$=9 Hz, 1H; H^5), 8.0 (t, $^3J_{H,H}$=7 Hz, 1H; H^{21}), 8.1–8.2 (m, 2H; H^3 and H^{20}), 8.2–8.3 (m, 2H; H^{14} and H^{19}), 8.3–8.4 (m, 3H; H^{10}, H^{12} and H^{13}), 8.6 (t, $^3J_{H,H}$=8.5 Hz, 1H; H^{22}), 9.2 (s, 1H; H^{24}), 9.8 ppm (s, 1H; H^{17}); MS (+FAB): *m*/*z* 562 [*M*$^+$]; elemental analysis calcd (%) for $C_{24}H_{15}ClN_2Pt$ (561.9): C 51.30, H 2.69, N 4.99; found: C 51.10, H 2.69, N 4.99.

[(*t*BuC^N^N)PtCl] (1b): K_2PtCl_4 (1.49 g, 3.58 mmol) and **b** (1.39 g, 3.58 mmol) were used. Complex **1b** was isolated as a yellow, crystalline solid. ^{1}H NMR spectroscopic data are not available due to the low solubility of **1b** in various deuterated solvents. Yield: 1.90 g (85.9%); MS (+FAB): *m*/*z* 618 [*M*$^+$]; elemental analysis calcd (%) for $C_{28}H_{23}ClN_2Pt$ (618.0): C 54.42, H 3.75, N 4.53; found: C 52.74, H 3.95, N 4.60.

[(PhC^N^N)PtCl] (1c): K_2PtCl_4 (0.52 g, 1.3 mmol) and **c** (0.51 g, 1.3 mmol) were used. Complex **1c** was isolated as yellow crystals. Yield: 0.72 g (90%); ^{1}H NMR (400 MHz, [D$_7$]DMF, 25°C, TMS): δ=7.4 (t, $^3J_{H,H}$=8 Hz, 1H; H^6), 7.4 (t, $^3J_{H,H}$=8 Hz, 1H; H^7), 7.6–7.7 (m, 3H; H^{10} and H^{26}), 7.7 (d, $^3J_{H,H}$=8 Hz, 1H; H^8), 7.8 (d, $^3J_{H,H}$=8 Hz, 1H; H^5), 7.9 (t, $^3J_{H,H}$=7 Hz, 1H, H^{21}), 8.0 (t, $^3J_{H,H}$=8 Hz, 1H; H^{20}), 8.1 (d, $^3J_{H,H}$= 8 Hz, 1H; H^{19}), 8.2 (m, 3H; H^{27} and H^{28}) 8.4–8.5 (m, 2H; H^{14} and H^{22}), 8.6 (s, 1H; H^{12}), 9.3 (s, 1H; H^{24}), 9.7 ppm (s, 1H; H^{17}); MS (+FAB): *m*/*z* 638 [*M*$^+$]; elemental analysis calcd (%) for $C_{30}H_{19}ClN_2Pt$ (638.0): C 56.48, H 3.00, N 4.39; found: C 56.04, H 3.02, N 4.50.

[(3,5-*t*Bu$_2$PhC^N^N)PtCl] (1d): K_2PtCl_4 (0.50 g, 1.2 mmol) and **d** (0.63 g, 1.2 mmol) were used. Complex **1d** was isolated as an orange, crystalline solid. Yield: 0.73 g (80%); ^{1}H NMR (400 MHz, [D$_7$]DMF, 25°C, TMS): δ=7.4 (t, $^3J_{H,H}$=7 Hz, 1H; H^6), 7.4 (t, $^3J_{H,H}$=6.7 Hz, 1H; H^7), 7.7 (d, $^3J_{H,H}$=7 Hz, 1H; H^8), 7.8 (m, 2H; H^5 and H^{28}), 7.9 (t, $^3J_{H,H}$=7 Hz, 1H; H^{21}), 8.0–8.1 (m, 5H; H^3, H^{19}, H^{20} and H^{26}), 8.4–8.5 (m, 3H; H^{10}, H^{14} and H^{22}), 8.6 (s, 1H; H^{12}), 9.3 (s, 1H; H^{24}), 9.7 ppm (s, 1H; H^{17}); MS (+FAB): *m*/*z* 751 [*M*$^+$]; elemental analysis calcd (%) for $C_{38}H_{35}ClN_2Pt$ (750.2): C 60.84, H 4.70, N 3.73; found: C 60.91, H 4.77, N 3.80.

[(3,5-F$_2$PhC^N^N)PtCl] (1e): K_2PtCl_4 (0.79 g, 1.9 mmol) and **e** (0.85 g, 1.9 mmol) were used. Complex **1e** was isolated as a yellow, crystalline solid. Yield: 1.1 g (88%); ^{1}H NMR (400 MHz, [D$_7$]DMF, 25°C, TMS): δ=7.3 (t, $^3J_{H,H}$=8 Hz, 1H; H^6), 7.3 (t, $^3J_{H,H}$=8 Hz, 1H; H^7), 7.5 (d, $^3J_{H,H}$=8 Hz, 1H; H^8), 7.6 (d, $^3J_{H,H}$=7.8 Hz, 1H; H^5), 7.7–7.8 (m, 4H; H^3 H^{21} and H^{26}), 7.9 (t, $^3J_{H,H}$=7 Hz, 1H; H^{20}), 8.0 (d, $^3J_{H,H}$=8 Hz, 1H; H^{19}), 8.1 (d, $^3J_{H,H}$=8 Hz, 1H; H^{22}), 8.2 (s, 2H; H^{10} and H^{12}), 8.42 (s, 1H; H^{14}), 9.04 (s, 1H; H^{24}), 9.29 ppm (s, 1H; H^{17}); ^{19}F NMR (376 MHz, [D$_7$]DMF, 25°C): δ=−110.13 ppm (t, $^3J_{H,F}$=8 Hz); MS (+FAB): *m*/*z* 674 [*M*$^+$]; elemental analysis calcd (%) for $C_{30}H_{17}ClF_2N_2Pt$ (674.0): C 53.46, H 2.54, N 4.16; found: C 53.14, H 2.42, N 4.47.

[(3,5-(CF$_3$)$_2$PhC^N^N)PtCl] (1f): K_2PtCl_4 (0.66 g, 1.6 mmol) and **f** (0.86 g, 1.6 mmol) were used. Complex **1f** was isolated as a yellow, crystalline solid. Yield: 1.1 g (92%); ^{1}H NMR spectroscopic data are not available because of the low solubility of **1f** in various deuterated solvents. ^{19}F NMR (376 MHz, [D$_7$]DMF, 25°C): δ=−62.1 ppm; MS (+FAB): *m*/*z* 774 [*M*$^+$]; elemental analysis calcd (%) for $C_{32}H_{17}ClF_6N_2Pt$ (774.0): C 49.66, H 2.21, N 3.62; found: C 49.67, H 2.01, N 3.72.

Synthesis of [(RC^N^N)$_2$Pt$_2$(μ-dppm)](ClO$_4$)$_2$ (2a–2f)

General procedure: dppm (0.55 equiv) was added to a solution of [(RC^N^N)PtCl] in an acetonitrile/dichloromethane mixture (40 mL, 1:1) with stirring. A clear yellow solution was obtained, to which an excess of $LiClO_4$ (10 equiv) was added. (**Caution!** *perchlorate salts are potentially explosive and should be handled with care and in small amounts*). The mixture was stirred at room temperature for 12 h, filtered and then concentrated on a rotary evaporator. Addition of diethyl ether gave the crude product as a bright yellow solid, which was washed with water and diethyl ether and recrystallized by diffusion of diethyl ether into an MeCN solution. Well-resolved ^{1}H NMR spectra for **2a–2f** can be obtained at −20 to −30°C. The structures and numbering scheme of **2a–2f** for NMR peak assignment are depicted in Figure 1.

[(HC^N^N)$_2$Pt$_2$(μ-dppm)](ClO$_4$)$_2$ (2a): Complex **1a** (0.10 g, 0.18 mmol), dppm (0.034 g, 0.089 mmol) and $LiClO_4$ (0.50 g, 4.7 mmol) gave **2a** as yellow crystals. Yield: 0.12 g (80%); ^{1}H NMR (500 MHz, CD_3CN, −30°C): δ=5.1 (t, $^2J_{H,P}$=13 Hz, 2H; PCH$_2$P), 5.6 (d, $^3J_{H,H}$=8 Hz, 2H; H^{22}), 6.4 (s, 2H; H^{17}), 6.8 (d, $^3J_{H,H}$=8 Hz, 2H; H^8), 6.9 (t, $^3J_{H,H}$=7 Hz, 2H; H^7), 7.0 (d, $^3J_{H,H}$=8 Hz, 2H; H^5), 7.0 (s, 2H; H^{10}), 7.1 (t, $^3J_{H,H}$= 7 Hz, 2H; H^{21}), 7.2–7.3 (m, 4H; H^3 and H^6), 7.6 (d, $^3J_{H,H}$=8 Hz, 2H; H^{12}), 7.7 (t, $^3J_{H,H}$=8 Hz, 2H; H^{20}), 7.8 (d, $^3J_{H,H}$=8 Hz, 2H; H^{14}), 7.9 (d, $^3J_{H,H}$=8 Hz, 2H; H^{19}), 8.0 (t, $^3J_{H,H}$=8 Hz, 2H; H^{13}), 8.3 ppm (s, 2H; H^{24}); the 20 protons of the phenyl rings in dppm: 7.0–7.1 (m, 2H), 7.2 (t, $^3J_{H,H}$=7 Hz, 2H), 7.4–7.5 (m, 4H), 7.6 (t, $^3J_{H,H}$=8 Hz, 2H), 7.7–7.8 (m, 4H), 8.2 (dd, $^3J_{H,H}$=8, $^3J_{H,P}$=14.2 Hz, 2H), 8.4 (t, $^3J_{H,H}$=9 Hz, 2H), 8.6 ppm (t, $^3J_{H,H}$=8 Hz, 2H); ^{31}P NMR (162 MHz, CD_3CN, 25°C): δ= 19.4 ppm ($^1J_{P,Pt}$=4138 Hz); MS (+FAB): *m*/*z* 1437 [*M*$^+$−2ClO$_4$]; elemental analysis calcd (%) for $C_{73}H_{52}Cl_2N_4O_8P_2Pt_2$ (1636.3): C 53.59, H 3.20, N 3.42; found: C 52.74, H 3.25, N 3.39.

[(*t*BuC^N^N)$_2$Pt$_2$(μ-dppm)](ClO$_4$)$_2$ (2b): Complex **1b** (0.10 g, 0.16 mmol), dppm (0.031 g, 0.081 mmol) and $LiClO_4$ (0.50 g, 4.7 mmol) gave **2b** as a yellow, crystalline solid. Yield: 0.098 g (70%); ^{1}H NMR (500 MHz, CD_3CN, −40°C): δ=1.5 (s, 18H; *t*Bu), 5.1 (d, $^3J_{H,H}$=8 Hz, 2H; H^{22}), 5.2 (t, $^2J_{H,P}$=12 Hz, 2H; PCH$_2$P), 6.5 (s, 2H; H^{17}), 7.0–7.1 (m, 8H; H^3, H^6, H^{10} and H^{21}), 7.2 (t, $^3J_{H,H}$=9 Hz, 2H; H^7), 7.3 (d, $^3J_{H,H}$= 8 Hz, 2H; H^5), 7.4; (d, $^3J_{H,H}$=8 Hz, 2H; H^8), 7.4 (s, 2H; H^{12}), 7.7 (s, 2H; H^{14}), 7.8 (t, $^3J_{H,H}$=8 Hz, 2H; H^{20}), 7.9 (d, $^3J_{H,H}$=8 Hz, 2H; H^{19}), 8.4 ppm (s, 2H; H^{24}); the 20 protons of the phenyl rings in dppm: 6.9 (t, $^3J_{H,H}$= 8 Hz, 2H), 7.0–7.1 (m, 2H), 7.3 (t, $^3J_{H,H}$=8 Hz, 2H), 7.5 (t, $^3J_{H,H}$=7 Hz, 2H), 7.6 (dd, $^3J_{H,H}$=7, $^3J_{H,P}$=14 Hz, 2H), 7.7 (t, $^3J_{H,H}$=8 Hz, 2H), 7.7–7.8 (m, 2H), 8.1 (dd, $^3J_{H,H}$=8, $^3J_{H,P}$=14 Hz, 2H), 8.4 (t, $^3J_{H,H}$=9 Hz, 2H), 8.6 ppm (t, $^3J_{H,H}$=9 Hz, 2H); ^{31}P NMR (162 MHz, CD_3CN, 25°C): δ= 18.0 ppm ($^1J_{P,Pt}$=4084 Hz). MS (+FAB): *m*/*z* 1550 [*M*$^+$−2ClO$_4$]; elemental analysis calcd (%) for $C_{81}H_{68}Cl_2N_4O_8P_2Pt_2$ (1748.5): C 55.64, H 3.92, N 3.20; found: C 54.85, H 4.01, N 3.85.

[(PhC^N^N)$_2$Pt$_2$(μ-dppm)](ClO$_4$)$_2$ (2c): Complex **1c** (0.15 g, 0.24 mmol), dppm (0.046 g, 0.12 mmol) and $LiClO_4$ (0.50 g, 4.7 mmol) gave **2c** as a yellow, crystalline solid. Yield: 0.19 g (86%); ^{1}H NMR (500 MHz, [D$_7$]DMF, −30°C): δ=5.6 (d, $^3J_{H,H}$=8 Hz, 2H; H^{22}), 5.9 (t, $^2J_{H,P}$=138 Hz, 2H; PCH$_2$P), 6.8 (s, 2H; H^{17}), 6.9 (d, $^3J_{H,H}$=8 Hz, 2H; H^8), 7.1 (t, $^3J_{H,H}$= 7 Hz, 2H; H^7), 7.2 (t, $^3J_{H,H}$=7 Hz, 2H; H^{21}), 7.3–7.4 (m, 6H; H^3, H^5 and H^6), 7.6 (t, $^3J_{H,H}$=8 Hz, 4H; H^{27}), 7.7 (t, $^3J_{H,H}$=7 Hz, 2H; H^{28}), 7.8 (s, 2H; H^{10}), 7.9–8.0 (m, 2H; H^{20}), 8.0 (d, $^3J_{H,H}$=8 Hz, 4H; H^{26}), 8.1 (d, $^3J_{H,H}$=8 Hz, 2H; H^{19}), 8.6 and 8.7 (2 s, 4H; H^{12} and H^{14}), 9.4 ppm (s, 2H; H^{24}); the 20 protons of the phenyl rings in dppm: 7.3–7.4 (m, 4H), 7.7 (t, $^3J_{H,H}$=7 Hz, 4H), 7.9–8.0 (m, 4H), 8.0–8.1 (m, 2H), 8.5 (t, 2H), 8.9 (t, $^3J_{H,H}$=8 Hz, 2H), 9.3 ppm (t, $^3J_{H,H}$=9 Hz, 2H); ^{31}P NMR (202 MHz, [D$_7$]DMF, 25°C): δ=20.2 ppm ($^1J_{P,Pt}$=4125 Hz); MS (+FAB): *m*/*z* 1590 [*M*$^+$−2ClO$_4$]; elemental analysis calcd (%) for $C_{85}H_{60}Cl_2N_4O_8P_2Pt_2$ (1788.5): C 57.09, H 3.38, N 3.13; found: C 56.28, H 3.41, N 3.51.

[(3,5-*t*Bu$_2$PhC^N^N)$_2$Pt$_2$(μ-dppm)](ClO$_4$)$_2$ (2d): Complex **1d** (0.12 g, 0.16 mmol), dppm (0.032 g, 0.083 mmol) and $LiClO_4$ (0.50 g, 4.7 mmol) gave **2d** as a yellow, crystalline solid. Yield: 0.13 g (78%); ^{1}H NMR (500 MHz, CD_2Cl_2, −40°C): δ=1.3 (s, 36H; *t*Bu), 5.0 (t, $^2J_{H,P}$=13 Hz, 2H; PCH$_2$P), 6.2 (d, $^3J_{H,H}$=11 Hz, 2H; H^{22}), 6.2 (s, 2H; H^{17}), 6.3 (t, $^3J_{H,H}$=7 Hz, 2H; H^6), 6.8 (d, $^3J_{H,H}$=8 Hz, 2H; H^8), 6.9 (m, 4H; H^5 and H^7), 7.1 (s, 2H; H^3), 7.3 (t, $^3J_{H,H}$=8 Hz, 2H; H^{21}), 7.4 (s, 4H; H^{26}), 7.5 (s, 2H; H^{28}), 7.7 (t, *J*=8 Hz, 2H; H^{20}), 7.8 (s, 2H; H^{10}), 7.9 (s, 2H; H^{12}), 8.0 (d, $^3J_{H,H}$=8 Hz, 2H; H^{19}), 8.3 (s, 2H; H^{14}), 8.7 ppm (s, 2H; H^{24}); the 20 protons of the phenyl rings in dppm: 7.2–7.3 (m, 6H), 7.6 (t, $^3J_{H,H}$=7 Hz, 2H), 7.7 (t, $^3J_{H,H}$=8 Hz, 2H), 7.8 (t, $^3J_{H,H}$=8 Hz, 2H), 7.9 (t, $^3J_{H,H}$=8 Hz, 2H), 8.3 (t, $^3J_{H,H}$=8 Hz, 2H), 8.4 (dd, $^3J_{H,H}$=8, $^3J_{H,P}$=14 Hz, 2H), 8.5 ppm (t, $^3J_{H,H}$=9 Hz, 2H); ^{31}P NMR (162 MHz, CD_2Cl_2, 25°C): δ= 19.4 ppm ($^1J_{P,Pt}$=4150 Hz); MS (+FAB): *m*/*z* 1914 [*M*$^+$−ClO$_4$], 1814 [*M*$^+$−2ClO$_4$]; elemental analysis calcd (%) for $C_{101}H_{92}Cl_2N_4O_8P_2Pt_2$ (2012.9): C 60.27, H 4.61, N 2.78; found: C 59.92, H 4.64, N 3.15.

[(3,5-F$_2$PhC^N^N)$_2$Pt$_2$(μ-dppm)](ClO$_4$)$_2$ (2e): Complex **1e** (0.06 g, 0.09 mmol), dppm (0.018 g, 0.047 mmol) and $LiClO_4$ (0.50 g, 4.7 mmol) gave **2e** as a yellow, crystalline solid. Yield: 0.07 g (80%); ^{1}H NMR

(500 MHz, [D$_7$]DMF, −20 °C): δ = 5.9 (t, $^2J_{H,P}$ = 13 Hz, 2H; PCH_2P), 6.0 (d, $^3J_{H,H}$ = 8 Hz, 2H; H^{22}), 6.7(s, 2H; H^{17}), 6.8–6.9 (m, 4H; H^5 and H^6), 7.1 (t, $^3J_{H,H}$ = 7 Hz, 2H; H^7), 7.2 (d, $^3J_{H,H}$ = 8 Hz, 2H; H^8), 7.3–7.4 (m, 4H; H^3 and H^{21}), 7.62 (t, $^3J_{H,F}$ = 9 Hz, 2H; H^{28}), 7.9–8.0 (m, 6H; H^{20} and H^{26}), 8.0–8.1 (m, 4H; H^{10} and H^{19}), 8.7 (s, 2H; H^{12}), 8.8 (s, 2H; H^{14}), 9.3 ppm (s, 2H; H^{24}); the 20 protons of the phenyl rings in dppm: 7.3–7.40 (m, 4H), 7.7–7.8 (m, 6H), 7.9–8.0 (m, 2H), 8.0–8.1 (m, 2H), 8.5 (dd, $^3J_{H,H}$ = 8, $^3J_{H,P}$ = 15 Hz, 2H), 8.8 (t, $^3J_{H,H}$ = 9 Hz, 2H), 9.1 ppm (t, $^3J_{H,H}$ = 8.6 Hz, 2H); ^{19}F NMR (376 MHz, [D$_7$]DMF): δ = −109.2 ppm (d, $^3J_{H,F}$ = 8 Hz); ^{31}P NMR (202 MHz, [D$_7$]DMF): δ = 19.9 ppm ($^1J_{P,Pt}$ = 4070 Hz); MS (+FAB): *m*/*z* 1761 [M^+−ClO_4], 1661 [M^+−2ClO_4]; elemental analysis calcd (%) for $C_{85}H_{56}Cl_2F_4N_4O_8P_2Pt_2$ (1860.4): C 54.88, H 3.03, N 3.01; found: C 53.94, H 3.32, N 3.83.

[(3,5-(CF$_3$)$_2$PhC^N^N)$_2$Pt$_2$(μ-dppm)](ClO$_4$)$_2$ (2f): Complex **1f** (0.15 g, 0.19 mmol), dppm (0.037 g, 0.10 mmol) and $LiClO_4$ (0.50 g, 4.7 mmol) were used to gave **2f** as an orange, crystalline solid. Yield: 0.18 g (90 %); ^{1}H NMR (500 MHz, [D$_7$]DMF, −30 °C): δ = 5.9 (t, $^2J_{H,P}$ = 13 Hz, 2H; PCH_2P), 6.4 (d, $^3J_{H,H}$ = 9 Hz, 2H; H^{22}), 6.4 (s, 2H; H^{17}), 6.5 (t, $^3J_{H,H}$ = 7 Hz, 2H; H^7), 6.7 (d, $^3J_{H,H}$ = 8 Hz, 2H; H^8), 7.0 (t, $^3J_{H,H}$ = 7 Hz, 2H; H^6), 7.2 (d, $^3J_{H,H}$ = 8 Hz, 2H; H^5), 7.5 (s, 2H; H^3), 7.5–7.6 (m, 4H; H^{19} and H^{21}), 8.0 (t, $^3J_{H,H}$ = 7.6 Hz, 2H; H^{20}), 8.2 (s, 2H; H^{10}), 8.45 (s, 2H; H^{28}), 8.8 (s, 4H; H^{26}), 9.0 (s, 2H; H^{12}), 9.1 (s, 2H; H^{14}), 9.2 ppm (s, 2H; H^{24}); the 20 protons of the phenyl rings in dppm: 7.4–7.5 (m, 4H), 7.5–7.6 (m, 2H), 7.8 (t, $^3J_{H,H}$ = 7 Hz, 2H), 7.84 (t, $^3J_{H,H}$ = 8 Hz, 2H), 7.9–8.0 (m, 2H), 8.0–8.1 (m, 2H), 8.6 (t, $^3J_{H,H}$ = 11 Hz, 2H), 8.8 (t, $^3J_{H,H}$ = 8 Hz, 2H), 9.1 ppm (t, $^3J_{H,H}$ = 11 Hz, 2H); ^{19}F NMR (376 MHz, [D$_7$]DMF, 25 °C): δ = −62.5 ppm; ^{31}P NMR (162 MHz, [D$_7$]DMF, 25 °C): δ = 19.9 ppm ($^1J_{P,Pt}$ = 4184 Hz); MS (+FAB): *m*/*z* 1962 [M^+−ClO_4], 1862 [M^+−2ClO_4]; elemental analysis calcd (%) for $C_{89}H_{56}Cl_2F_{12}N_4O_8P_2Pt_2$ (2060.4): C 51.88, H 2.74, N 2.72; found: C 51.76, H 2.88, N 2.87.

Synthesis of [(RC^N^N)PtX](ClO$_4$) (3c: X = PPh$_3$; 4b,4c: X = PCy$_3$)

General procedure: PPh_3 or PCy_3 was added to a solution of the corresponding [(RC^N^N)PtCl] complex in a mixture of MeCN (20 mL) and CH_2Cl_2 (20 mL) whilst stirring. Excess $LiClO_4$ was then added to the clear yellow solution. (***Caution!*** *Perchlorate salts are potentially explosive and should be handled with care in small amounts.*) After stirring at room temperature for 12 h, the mixture was filtered and the filtrate was concentrated. Addition of diethyl ether to the concentrated filtrate gave the crude product as a bright yellow solid, which was washed with water and diethyl ether. The solid was recrystallized by vapor diffusion of diethyl ether into a MeCN solution.

[(PhC^N^N)PtPPh$_3$](ClO$_4$) (3c): A mixture of **1c** (0.10 g, 0.15 mmol), PPh_3 (0.04 g, 0.2 mmol) and excess $LiClO_4$ (0.50 g, 4.7 mmol) in MeCN/CH_2Cl_2 gave **3c** as yellow crystals. Yield: 0.10 g (80 %); ^{1}H NMR (400 MHz, [D$_7$]DMF, 25 °C): δ = 6.9 (d, $^3J_{H,H}$ = 8 Hz, 1H; H^{22}), 6.9 (s, 1H; H^{19}), 7.3–7.4 (m, 3H; H^8, H^{20} and H^{21}), 7.5 (s, 1H; H^3), 7.6–7.7 (m, 9H; *m*-Ph, H^{27} and H^{28}), 7.7 (t, $^3J_{H,H}$ = 9 Hz, 3H; *p*-Ph), 7.8 (d, $^3J_{H,H}$ = 9 Hz, 1H; H^{19}), 7.9 (t, $^3J_{H,H}$ = 8 Hz, 1H; H^6), 8.1 (t, $^3J_{H,H}$ = 8 Hz, 1H; H^7), 8.1–8.2 (m, 7H; H^5 and *o*-Ph), 8.3 (d, $^3J_{H,H}$ = 10 Hz, 2H; H^{26}), 8.8 (s, 1H; H^{24}), 8.9 (s, 1H; H^{12}), 9.0 (s, 1H; H^{14}), 9.5 ppm (s, 1H; H^{10}); MS (+FAB): *m*/*z* 864 [M^+−ClO_4]; elemental analysis calcd (%) for $C_{48}H_{34}ClN_2O_4PPt$ (964.3): C 59.79, H 3.55, N 2.91; found: C, 58.88, H 3.48, N 3.05.

[(*t*BuC^N^N)PtPCy$_3$](ClO$_4$) (4b): A mixture of **1b** (0.03 g, 0.05 mmol), PCy_3 (0.015 g, 0.054 mmol) and excess $LiClO_4$ (0.50 g, 4.7 mmol) in MeCN/CH_2Cl_2 gave **4b** as yellow crystals. Yield: 0.03 g (60 %); ^{1}H NMR (300 MHz, CD_3CN, 25 °C): δ = 1.1–1.3 (m, 9H; Cy), 1.6 (s, 9H; *t*Bu), 1.6–1.8 (m, 15H; Cy), 2.2–2.3 (m, 6H; Cy), 2.7–2.8 (m, 3H; Cy), 7.4–7.6 (m, 2H; H^{20} and H^{21}), 7.8 (d, $^3J_{H,H}$ = 7.9 Hz, 1H; H^{19}), 7.9 (d, $^3J_{H,H}$ = 8 Hz, 1H; H^{22}), 7.9–8.0 (m, 2H; H^7 and H^{24}), 8.1 (t, $^3J_{H,H}$ = 5 Hz, 1H; H^6), 8.2–8.3 (m, 3H; H^5, H^{12} and H^{14}), 8.4 (s, 1H; H^{17}), 8.5 (d, $^3J_{H,H}$ = 8 Hz, 1H; H^8), 9.0 (s, 1H; H^{10}), 9.6 ppm (s, 1H; H^3); MS (+FAB): *m*/*z* 863 [M^+−ClO_4]; elemental analysis calcd (%) for $C_{46}H_{56}ClN_2O_4PPt{\cdot}2CH_3CN$ (1044.6): C 57.49, H 5.98, N 5.36; found: C 56.99, H 5.92, N 5.06.

[(PhC^N^N)PtPCy$_3$](ClO$_4$) (4c): A mixture of **1c** (0.10 g, 0.15 mmol), PCy_3 (0.04 g, 0.1 mmol) and excess $LiClO_4$ (0.50 g, 4.7 mmol) in MeCN/CH_2Cl_2 gave **4c** as yellow crystals. Yield: 0.098 g (75 %); ^{1}H NMR (400 MHz, CD_3CN, 25 °C): δ = 1.1–1.3 (m, 9H; Cy), 1.6–1.7 (m, 15H; Cy), 2.1–2.2 (m, 6H; Cy), 2.6–2.7 (m, 3H; Cy), 7.3–7.4 (m, 2H; H^{20} and H^{21}), 7.5–7.56 (m, 3H; H^{27} and H^{28}), 7.6–7.7 (m, 1H; H^{22}), 7.7 (s, 1H; H^{12}), 7.7–7.8 (m, 1H; H^{19}), 7.8–7.9 (m, 3H; H^7 and H^{26}), 8.0 (t, $^3J_{H,H}$ = 8 Hz, 1H; H^6), 8.1 (s, 1H; H24), 8.1 (d, $^3J_{H,H}$ = 7 Hz, 1H; H^5), 8.2 (s, 1H; H^{14}), 8.2 (d, $^3J_{H,H}$ = 8 Hz, 1H; H^8), 8.3 (s, 1H; H^{17}), 8.8 (s, 1H; H^{10}), 9.4 ppm (s, 1H; H^3); MS (+FAB): *m*/*z* 882 [M^+−ClO_4]; elemental analysis calcd (%) for $C_{48}H_{52}ClN_2O_4PPt$ (982.5): C 58.68, H 5.33, N 2.85; found: C 58.68, H 5.49, N 3.29.

Synthesis of [(RC^N^N)$_3$Pt$_3$(μ-dpmp)](ClO$_4$)$_3$ (5b and 5d)

General procedure: dpmp (0.33 equiv) was added to a solution of [(RC^N^N)PtCl] in an acetonitrile/dichloromethane mixture (10 mL, 1:1) whilst stirring. A clear orange solution was obtained, to which excess $LiClO_4$ (10 equiv) was added. (***Caution!*** *Perchlorate salts are potentially explosive and should be handled with care and in small amounts*). The mixture was stirred at room temperature for 12 h, filtered and concentrated. Addition of diethyl ether gave the crude product as a bright yellow solid, which was washed with water and diethyl ether and recrystallized by diffusion of diethyl ether into an acetonitrile solution. Since there are many non-equivalent protons in **5b** and **5d**, the peaks in the aromatic region of their ^{1}H NMR spectra were not assigned.

[(*t*BuC^N^N)$_3$Pt$_3$(μ-dpmp)](ClO$_4$)$_3$ (5b): Complex **1b** (0.063 g, 0.10 mmol), dpmp (0.017 g, 0.034 mmol) and $LiClO_4$ (0.5 g, 4.7 mmol) gave **5b** as a yellow, crystalline solid. Yield: 0.077 g (88 %); ^{1}H NMR (400 MHz, CD_2Cl_2, 24 °C): δ = 1.3 (s, 9H, *t*Bu(central)), 1.5 ppm (s, 18H, *t*Bu(terminal)); protons in the aromatic region were not assigned; ^{31}P NMR (162 MHz, CD_2Cl_2, 24 °C): δ = 8.8 ($^1J_{P,Pt}$ = 4150 Hz, central), 10.7 ppm ($^1J_{P,Pt}$ = 4057 Hz, terminal); ^{195}Pt NMR (107 MHz, CD_2Cl_2, 24 °C): δ = −3917.0 (d, $^1J_{P,Pt}$ = 3959, terminal), −3779.7 ppm (d, $^1J_{P,Pt}$ = 3980, central); MS (+FAB): *m*/*z* 2250 [M^+−3ClO_4]; elemental analysis calcd (%) for $C_{116}H_{98}Cl_3N_6O_{12}P_3Pt_3$ (2552.6): C 54.58, H 3.87, N 3.29; found: C 54.23, H 3.52, N 3.12.

[(3,5-*t*Bu$_2$PhC^N^N)$_3$Pt$_3$(μ-dpmp)](ClO$_4$)$_3$ (5d): Complex **1d** (0.1 g, 0.133 mmol), dpmp (0.022 g, 0.044 mmol) and $LiClO_4$ (0.5 g, 4.7 mmol) gave **5d** as an orange, crystalline solid. Yield: 0.28 g (71 %); ^{1}H NMR (400 MHz, CD_2Cl_2, 24 °C): δ = 1.2 (s, 18H; *t*Bu(central)), 1.3 ppm (s, 36H; *t*Bu(terminal)); protons in the aromatic region were not assigned; ^{31}P NMR (162 MHz, CD_2Cl_2, 24 °C): δ = 9.7 ($^1J_{P,Pt}$ = 4042 Hz, central), 11.7 ppm ($^1J_{P,Pt}$ = 4094 Hz, terminal); ^{195}Pt NMR (107 MHz, CD_2Cl_2, 24 °C): δ = −3886.5 (d, $^1J_{P,Pt}$ = 4070, terminal), −3727.8 ppm (d, $^1J_{P,Pt}$ = 3995, central); MS (+FAB): *m*/*z* 2650 [M^+−3ClO_4]; elemental analysis calcd (%) for $C_{146}H_{134}Cl_3N_6O_{12}P_3Pt_3$ (2949.2): C 59.46, H 4.58, N 2.85; found: C 59.11, H 4.65, N 2.73.

X-ray crystallography: Crystals were mounted either inside a sealed capillary or on a thin glass fibre. Intensity data were collected at −20 °C on a MAR diffractometer with a 300-mm image plate detector using graphite-monochromated Mo-K_α radiation (λ = 0.71073 Å). The images were interpreted and intensity was integrated with the program DENZO.[63] All structures were solved by direct methods implemented in the SIR-97[64] program on a PC. The heavy atoms (such as Pt and P) were initially located in the partial structure solution from Fourier syntheses. The positions of other non-hydrogen atoms were located after a few cycles of refinement based on full-matrix least-squares of $|F^2|$ using the SHELXL-97 program suite.[65] Solvent molecules and/or perchlorate anions in **1a**, **1c**, **2a**–**2d**, **2f**, **3c**, **4b**, **4c** and **5b** were found to be disordered and split occupancy factors (55:45) were assigned to each component of the same constrained thermal parameters. C−Cl distances of 1.720 ± 0.005 Å were applied to all the $CHCl_3$ and CH_2Cl_2 molecules. The positions of all aromatic hydrogen atoms were calculated from the idealized restrained positions (a riding model) with a fixed C–H distance of 0.96 Å. Isotropic thermal parameters of all hydrogen atoms were constrained to the value of 1.2-times those of the attached carbons.

Organic-light emitting devices (OLEDs): The electroluminescent (EL) devices were prepared on patterned indium-tin-oxide (ITO) glass with a sheet resistance of 20 Ω/□. Thermal vacuum deposition of the materials was carried out sequentially under a vacuum of 1×10^{-6} Torr in a thin-film deposition system (an MBraun three-glove box system integrated with an Edwards Auto 306 and spin coater instrument). The devices were encapsulated using anodized aluminum caps and their performance was

examined with a Photoresearch PR-650. The current–voltage characteristics were studied with a Keithley 2400 sourcemeter.

Acknowledgments

We gratefully acknowledge financial support by the University Development Fund (Nanotechnology Research Institute, 00600009) of The University of Hong Kong, Research Grants Council of HKSAR, China (HKU 7039/03P), Innovation and Technology Commission of the HKSAR Government (ITF GHP/062/05) and National Science Foundation of China/Research Grants Council Joint Research Scheme (N_HKU 742/04).

[1] S. W. Lai, C. M. Che, *Topics in Current Chemistry, Vol. 241: Transition Metal and Rare Earth Compounds III: Excited States, Transitions, Interactions* (Ed.: H. Yersin), Springer, New York, **2004**, pp. 27–63.
[2] C. E. Whittle, J. A. Weinstein, M. W. George, K. S. Schanze, *Inorg. Chem.* **2001**, *40*, 4053–4062.
[3] M. Hissler, J. E. McGarrah, W. B. Connick, D. K. Geiger, S. D. Cummings, R. Eisenberg, *Coord. Chem. Rev.* **2000**, *208*, 115–137.
[4] B. Ma, J. Li, P. I. Djurovich, M. Yousufuddin, R. Bau, M. E. Thompson, *J. Am. Chem. Soc.* **2005**, *127*, 28–29.
[5] C. Yu, K. M. C. Wong, K. H. Y. Chan, V. W. W. Yam, *Angew. Chem.* **2005**, *117*, 801–804; *Angew. Chem. Int. Ed.* **2005**, *44*, 791–794.
[6] S. D. Cummings, R. Eisenberg, *J. Am. Chem. Soc.* **1996**, *118*, 1949–1960.
[7] W. B. Connick, V. M. Miskowski, V. H. Houlding, H. B. Gray, *Inorg. Chem.* **2000**, *39*, 2585–2592.
[8] V. M. Miskowski, V. H. Houlding, *Inorg. Chem.* **1991**, *30*, 4446–4452.
[9] H. K. Yip, C. M. Che, Z. Y. Zhou, T. C. W. Mak, *J. Chem. Soc. Chem. Commun.* **1992**, 1369–1371.
[10] V. M. Miskowski, V. H. Houlding, C. M. Che, Y. Wang, *Inorg. Chem.* **1993**, *32*, 2518–2524.
[11] C. W. Chan, L. K. Cheng, C. M. Che, *Coord. Chem. Rev.* **1994**, *132*, 87–97.
[12] S. W. Lai, M. C. W. Chan, K. K. Cheung, C. M. Che, *Inorg. Chem.* **1999**, *38*, 4262–4267.
[13] S. W. Lai, M. C. W. Chan, T. C. Cheung, S. M. Peng, C. M. Che, *Inorg. Chem.* **1999**, *38*, 4046–4055.
[14] B. C. Tzeng, S. C. Chan, M. C. W. Chan, C. M. Che, K. K. Cheung, S. M. Peng, *Inorg. Chem.* **2001**, *40*, 6699–6704.
[15] W. Lu, B. X. Mi, M. C. W. Chan, Z. Hui, N. Zhu, S. T. Lee, C. M. Che, *Chem. Commun.* **2002**, 206–207.
[16] W. Lu, M. C. W. Chan, N. Zhu, C. M. Che, C. Li, Z. Hui, *J. Am. Chem. Soc.* **2004**, *126*, 7639–7651.
[17] J. A. Bailey, V. M. Miskowski, H. B. Gray, *Inorg. Chem.* **1993**, *32*, 369–370.
[18] L. Z. Wu, T. C. Cheung, C. M. Che, K. K. Cheung, M. H. W. Lam, *Chem. Commun.* **1998**, 1127–1128.
[19] W. Lu, B. X. Mi, M. C. W. Chan, Z. Hui, C. M. Che, N. Zhu, S. T. Lee, *J. Am. Chem. Soc.* **2004**, *126*, 4958–4971.
[20] T. C. Cheung, K. K. Cheung, S. M. Peng, C. M. Che, *J. Chem. Soc. Dalton Trans.* **1996**, 1645–1651.
[21] C. W. Chan, T. F. Lai, C. M. Che, S. M. Peng, *J. Am. Chem. Soc.* **1993**, *115*, 11245–11253.
[22] L. Chassot, A. Von Zelewsky, D. Sandrini, M. Maestri, V. Balzani, *J. Am. Chem. Soc.* **1986**, *108*, 6084–6085.
[23] M. Maestri, D. Sandrini, V. Balzani, A. Von Zelewsky, P. Jolliet, *Helv. Chim. Acta* **1988**, *71*, 134–139.
[24] M. Maestri, C. Deuschel-Cornioley, A. Von Zelewsky, *Coord. Chem. Rev.* **1991**, *111*, 117–123.
[25] S. C. F. Kui, S. S. Y. Chui, C. M. Che, N. Zhu, *J. Am. Chem. Soc.* **2006**, *128*, 8297–8309.
[26] F. Barigelletti, B. Ventura, J.-P. Collin, R. Kayhanian, P. Gavina, J.-P. Sauvage, *Eur. J. Inorg. Chem.* **2000**, 113–119.
[27] E. C. Constable, R. P. G. Henney, T. A. Leese, D. A. Tocher, *J. Chem. Soc. Dalton Trans.* **1990**, 443–449.
[28] W. Lu, M. C. W. Chan, K. K. Cheung, C. M. Che, *Organometallics* **2001**, *20*, 2477–2486.
[29] P. H. M. Budzelaar, *gNMR version 4.1.0.*, Cherwell Scientific Publishing, **1999**.
[30] CCDC-287984–287992, CCDC-601687, and CCDC-601688 contain the supplementary crystallographic data for **1c**, **2a**–**2d**, **2f**, **3c**, **4b**, **4c**, **1a**, and **5b**, respectively. These data can be obtained free of charge via www. ccdc.cam.ac.uk/data_request/cif.
[31] D. A. Bardwell, J. G. Crossley, J. C. Jeffery, A. G. Orpen, E. Psillakis, E. E. M. Tilley, M. D. Ward, *Polyhedron* **1994**, *13*, 2291–2300.
[32] C. C. Kwok, H. M. Y. Ngai, S. C. Chan, I. H. T. Sham, C. M. Che, N. Zhu, *Inorg. Chem.* **2005**, *44*, 4442–4444.
[33] Y. Y. Lin, S. C. Chan, M. C. W. Chan, Y. J. Hou, N. Zhu, C. M. Che, Y. Liu, Y. Wang, *Chem. Eur. J.* **2003**, *9*, 1263–1272.
[34] C. Janiak, *J. Chem. Soc. Dalton Trans.* **2000**, 3885–3896.
[35] C. A. Hunter, J. K. M. Sanders, *J. Am. Chem. Soc.* **1990**, *112*, 5525–5534.
[36] C. M. Che, L. Y. He, C. K. Poon, T. C. W. Mak, *Inorg. Chem.* **1989**, *28*, 3081–3083.
[37] A. F. Stange, T. Sixt, W. Kaim, *Chem. Commun.* **1998**, 469–470.
[38] K. T. Wan, C. M. Che, K. C. Cho, *J. Chem. Soc. Dalton Trans.* **1991**, 1077–1080.
[39] J. A. Bailey, M. G. Hill, R. E. Marsh, V. M. Miskowski, W. P. Schaefer, H. B. Gray, *Inorg. Chem.* **1995**, *34*, 4591–4599.
[40] V. H. Houlding, V. M. Miskowski, *Coord. Chem. Rev.* **1991**, *111*, 145–152.
[41] C. M. Che, S. C. Chan, H. F. Xiang, M. C. W. Chan, Y. Liu, Y. Wang, *Chem. Commun.* **2004**, 1484–1485.
[42] I. R. Laskar, S.-F. Hsu, T.-M. Chen, *Polyhedron* **2005**, *24*, 881–888.
[43] S.-Y. Chang, J. Kavitha, S.-W. Li, C.-S. Hsu, Y. Chi, Y.-S. Yeh, P.-T. Chou, G.-H. Lee, A. J. Carty, Y.-T. Tao, C.-H. Chien, *Inorg. Chem.* **2006**, *45*, 137–146.
[44] X. Q. Lin, B. J. Chen, X. H. Zhang, C. S. Lee, H. L. Kwong, S. T. Lee, *Chem. Mater.* **2001**, *13*, 456–458.
[45] M. Mazzeo, D. Pisignano, L. Favaretto, G. Barbarella, R. Cingolani, G. Gigli, *Synth. Met.* **2003**, *139*, 671–673.
[46] S. Lamansky, P. Djurovich, D. Murphy, F. Abdel-Razzaq, H. E. Lee, C. Adacjo, P. E. Burrows, S. R. Forrest, M. E. Thompson, *J. Am. Chem. Soc.* **2001**, *123*, 4304–4312.
[47] W. Sotoyama, T. Satoh, N. Sawatari, H. Inoue, *Appl. Phys. Lett.* **2005**, *86*, 153505/1–153505/3.
[48] H. F. Xiang, S. C. Chan, K. K. Y. Wu, C. M. Che, P. T. Lai, *Chem. Commun.* **2005**, 1408–1410.
[49] J. Kavitha, S.-Y. Chang, Y. Chi, J.-K. Yu, Y.-H. Hu, P.-T. Chou, S.-M. Peng, G.-H. Lee, Y.-T. Tao, C.-H. Chien, A. J. Carty, *Adv. Funct. Mater.* **2005**, *15*, 223–229.
[50] W.-Y. Wong, Z. He, S.-K. So, K.-L. Tong, Z. Lin, *Organometallics* **2005**, *24*, 4079–4082.
[51] M. Cocchi, V. Fattori, D. Virgili, C. Sabatini, P. Di Marco, M. Maestri, J. Kalinowski, *Appl. Phys. Lett.* **2004**, *84*, 1052–1054.
[52] B. W. D′Andrade, J. Brooks, V. Adamovich, M. E. Thompson, S. R. Forrest, *Adv. Mater.* **2002**, *14*, 1032–1036.
[53] S. C. Chan, M. C. W. Chan, Y. Wang, C. M. Che, K. K. Cheung, N. Zhu, *Chem. Eur. J.* **2001**, *7*, 4180–4190.
[54] G. F. Strouse, J. R. Schoonover, R. Duesing, S. Boyde, W. E. J. Jones, T. J. Meyer, *Inorg. Chem.* **1995**, *34*, 473–487.
[55] D. D. Perrin, W. L. F. Armarego, D. R. Perrin, *Purification of Laboratory Chemicals*, 2nd ed. Pergamon, Oxford, **1980**.
[56] J. Y. Legros, G. Primault, J. C. Fiaud, *Tetrahedron* **2001**, *57*, 2507–2514.
[57] R. G. Pearson, *J. Am. Chem. Soc.* **1947**, *69*, 3100–3103.
[58] L. C. King, M. McWhirter, R. L. Rowland, *J. Am. Chem. Soc.* **1948**, *70*, 239–242.
[59] F. F. Blicke, J. H. Burckhalter, *J. Am. Chem. Soc.* **1942**, *64*, 451–454.

[60] G. W. V. Cave, C. L. Raston, *J. Chem. Soc. Perkin Trans. 1* **2001**, 3258–3264.
[61] F. Neve, A. Crispini, S. Campagna, *Inorg. Chem.* **1997**, *36*, 6150–6156.
[62] P. S. Kendurkar, R. S. Tewari, *J. Chem. Eng. Data* **1974**, *19*, 184–188.
[63] DENZO: In the HKL Manual—A description of programs DENZO, XDISPLAYF and SCALEPACK; written by D. Gewirth with the cooperation of the program authors Z. Otwinowski and W. Minor; Yale University: New Haven, CT (USA), **1995**.
[64] A. Altomare, M. C. Burla, M. Camalli, G. L. Cascarano, C. Giacovazzo, A. Guagliardi, A. G. G. Moliterni, G. Polidori, R. Spagna, *J. Appl. Crystallogr.* **1999**, *32*, 115–119.
[65] G. M. Sheldrick, SHELXS-97, Programs for Crystal Structure Analysis (Release 97-2), University of Göttingen, Germany, **1997**.

Received: May 17, 2006
Revised: June 23, 2006
Published online: November 30, 2006

